The Failure of U-Th-Pb 'Dating' at Koongarra, Australia

DR ANDREW A. SNELLING

ABSTRACT

As with other radiometric 'dating' methods, the U-Pb and Pb-Pb isochron methods have been questioned in the open literature, because often an excellent line of best fit between ratios obtained from a set of good cogenetic samples gives a resultant 'isochron' and yields a derived 'age' that has no geological meaning. At the Koongarra uranium deposit, Australia, there is ample evidence of open system behaviour, or repeated migration, of U and Pb — ore textures, mineral chemistry, supergene alteration, uranium/daughter disequilibrium, and groundwater and soil geochemistry. Yet U-Th-Pb isotopic studies of the uranium ore, host rocks and soils have produced an array of false 'isochrons' that yield 'ages' which are geologically meaningless. Even a claimed near-concordant U-Pb 'age' of 862 Ma (million years) on one uraninite grain is identical to a false Pb-Pb isochron 'age', but neither can be connected to any geological event. The open system behaviour of the U-Th-Pb system is clearly the norm, as is the resultant mixing of radiogenic Pb with 'common' or background Pb, even in soils in the surrounding region, apparently even up to 17 km away! Because no geologically meaningful results can be interpreted from the U-Th-Pb data at Koongarra (three uraninite grains even yield a $^{232}Th/^{208}Pb$ 'age' of 0 Ma), serious questions must be asked about the validity of the fundamental/foundational basis of the U-Th-Pb 'dating' method. This makes the task of creationists building their model for the geological record much easier, since claims of U-Th-Pb radiometric 'dating' having 'proven' the claimed great antiquity of the earth, its strata and fossils can be justifiably ignored.

INTRODUCTION

Radiometric dating has now been used for almost 50 years to establish 'beyond doubt' the multi-billion year age of the earth's geological column. Although this column and its 'age' was firmly settled well before the advent of radiometric dating, the latter has been used to quantify the 'ages' of the strata and the fossils in the column, so that in many people's minds today radiometric dating has 'proved' the presumed antiquity of the earth.

However, it is important to remember that **all** radiometric dating methods are based on three main assumptions:–

(1) The physico-chemical system must have always been closed. Thus no parent, daughter or other decay products within the system can have been removed, and no parent, daughter or other decay products from outside the system can have been added.
(2) The system must initially have contained none of its daughter elements or decay products, or at the very least we need to know the starting conditions/state of the decay system.
(3) The decay rate, referred to as the half-life of the radioactive parent element, must have always been the same, that is, constant.

The highly speculative nature of all radiometric dating methods becomes apparent when one realizes that none of the above assumptions is either valid or provable. Put simply, none of these assumptions can have been **observed** to have **always** been true throughout the supposed millions of years the radioactive elements have presumed to have been

decaying.

Of the various radiometric methods, uranium-thorium-lead (U-Th-Pb) was the first used and it is still widely employed today, particularly when zircons are present in the rocks to be dated. But the method does not always give the 'expected' results, leading to fundamental questions about its validity. Indeed, the U-Th-Pb system is well known to be prone to open system behaviour, with U being particularly geochemically mobile, meaning that U is readily lost from the crystal lattices of the minerals used for 'dating', including zircons. Pb is also prone to diffusion from minerals. Thus it is questionable as to why this radiometric 'dating' method is still used. Instead, it is increasingly being applied in more sophisticated ways to geological 'dating' problems.

In the conclusion to a recent paper exposing shortcomings and criticising the validity of the popular rubidium-strontium (Rb-Sr) isochron method, Zheng wrote:

> *'. . . some of the basic assumptions of the conventional Rb-Sr isochron method have to be modified and an observed isochron does not certainly define a valid age information for a geological system, even if a goodness of fit of the experimental data points is obtained in plotting $^{87}Sr/^{86}Sr$ vs. $^{87}Rb/^{86}Sr$. This problem cannot be overlooked, especially in evaluating the numerical time scale. Similar questions can also arise in applying Sm-Nd and U-Pb isochron methods'*[1]

Amongst the concerns voiced by Zheng were the problems being found with anomalous isochrons, that is, where there is an apparent linear relationship between $^{87}Sr/^{86}Sr$ and $^{87}Rb/^{86}Sr$ ratios, even an excellent line of best fit between ratios obtained from good cogenetic samples, and yet the resultant isochron and derived 'age' have no distinct geological meaning. Zheng documented the copious reporting of this problem in the literature where various names had been given to these anomalous isochrons, such as apparent isochron, mantle isochron and pseudoisochron, secondary isochron, inherited isochron, source isochron, erupted isochron, mixing line, and mixing isochron.

Similar anomalous or false isochrons are commonly obtained from U-Th-Pb data, which is hardly surprising given the common open system behaviour of the U-Th-Pb system. Yet in the literature these problems are commonly glossed over or pushed aside, but their increasing occurrence from a variety of geological settings does seriously raise the question as to whether U-Th-Pb data ever yields any valid 'age' information. One such geological setting that yields these false U-Th-Pb 'ages' and 'isochrons' is the Koongarra uranium deposit and the surrounding area (Northern Territory, Australia).

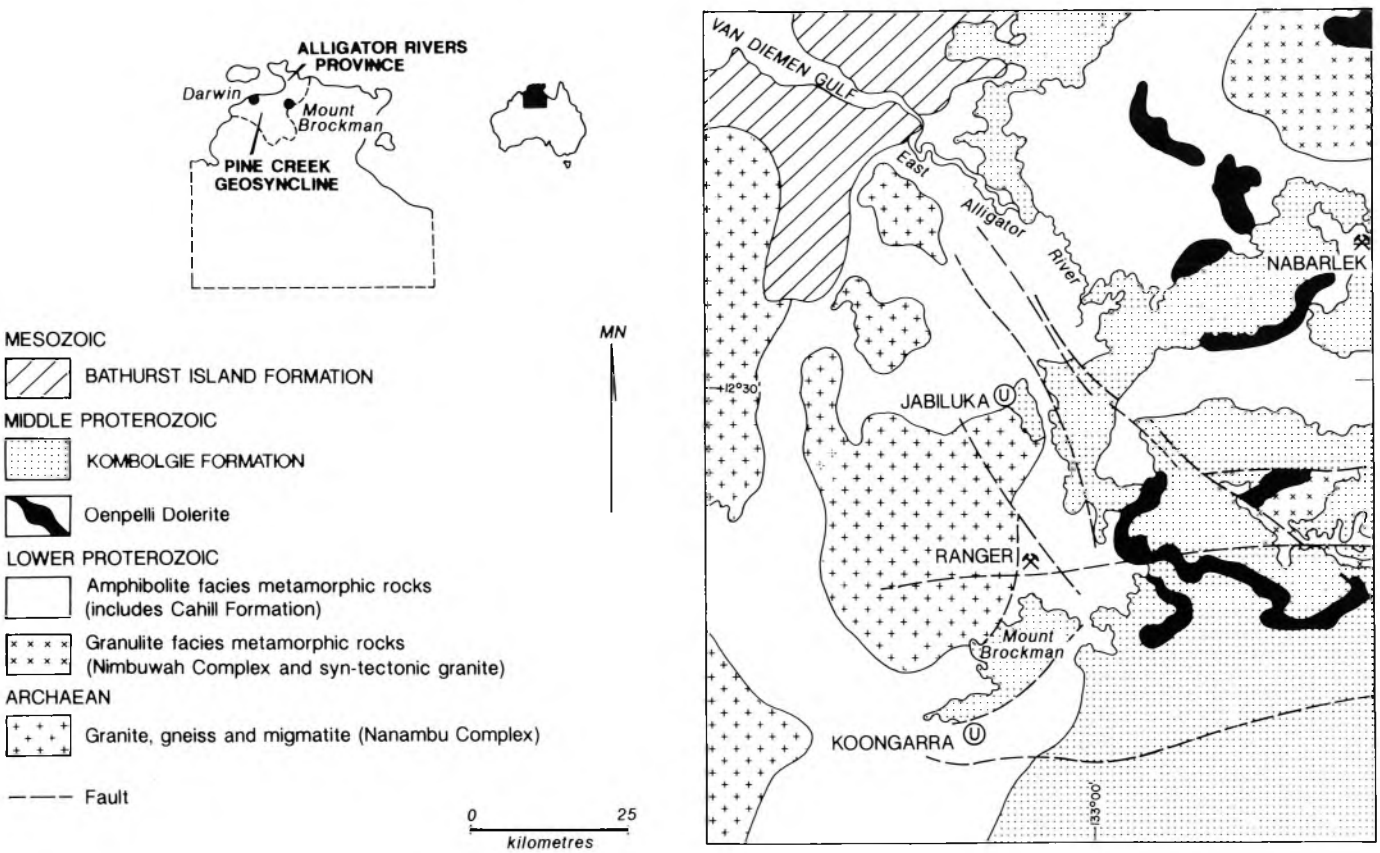

Figure 1. *Regional geology map showing the location of the Koongarra uranium deposit.*

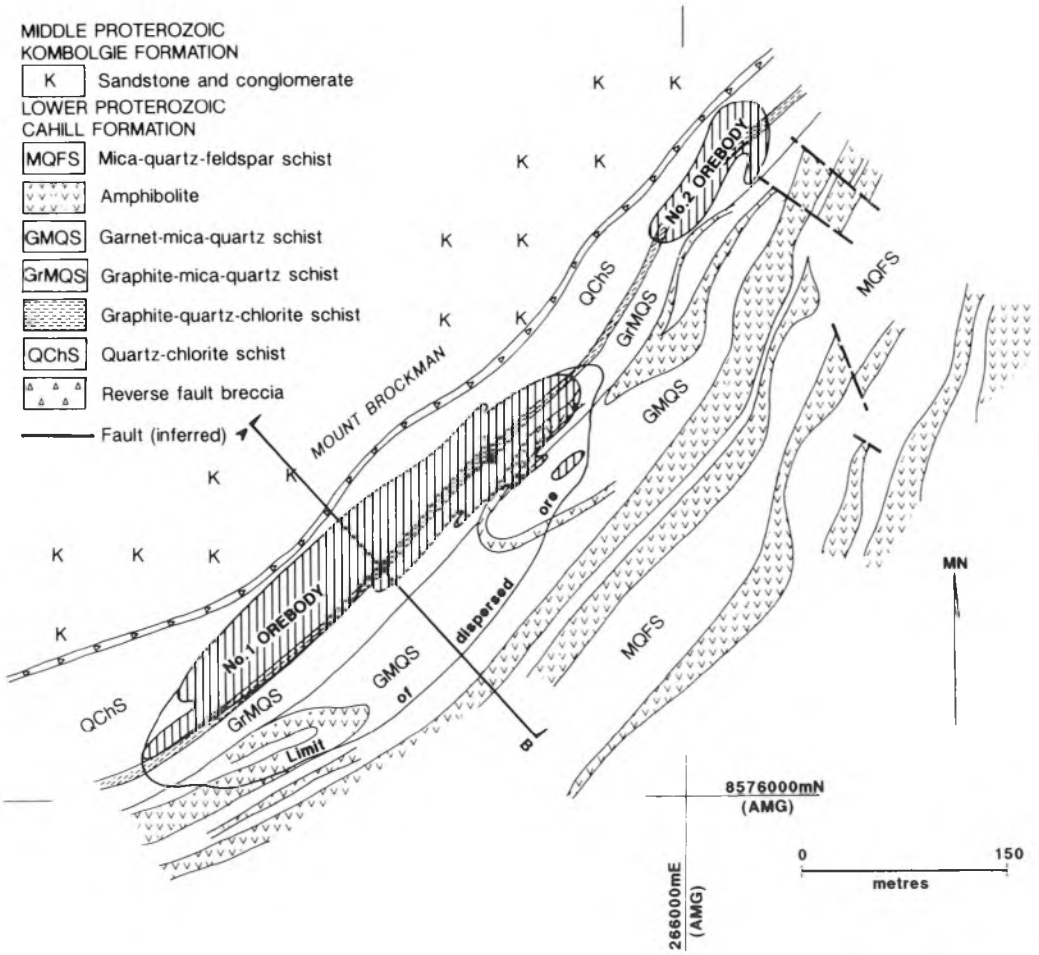

Figure 2. *Local geology map showing the location of the Koongarra No. 1 and No. 2 orebodies. Because of surficial cover the geological units and outline of the mineralisation are projected to the surface from the base of weathering.*

THE KOONGARRA AREA

The Koongarra area is 250 km east of Darwin (Northern Territory, Australia) at latitude 12°52'S and longitude 132°50'E. The regional geology has been described in detail by Needham and Stuart-Smith[2] and by Needham[3,4] (see Figure 1), while Snelling[5] describes the Koongarra uranium deposit and the area's local geology (see Figure 2).

The Koongarra uranium deposit occurs in a metamorphic terrain that has an Archaean basement consisting of domes of granitoids and granitic gneisses (the Nanambu Complex), the nearest outcrop being 5 km to the north (see Figure 1). Some of the lowermost overlying Lower Proterozoic metasediments were accreted to these domes during amphibolite grade regional metamorphism (estimated to represent conditions of 5–8 kb and 550–630° C) at 1800–1870 Ma (million years ago, according to conventional evolutionary dating). Multiple isoclinal recumbent folding accompanied metamorphism. The Lower Proterozoic Cahill Formation flanking the Nanambu Complex has been divided into two members. The lower member is dominated by a thick basal dolomite and passes transitionally upwards into the psammitic upper member, which is largely feldspathic schist and quartzite. The uranium mineralisation at Koongarra is associated with graphitic horizons within chloritised quartz-mica (±feldspar ±garnet) schists overlying the basal dolomite in the lower member (see Figures 2 and 3). A 150 Ma period of weathering and erosion followed metamorphism. A thick sequence of essentially flat-lying sandstones (the Middle Proterozoic Kombolgie Formation) was then deposited unconformably on the Archaean-Lower Proterozoic basement and metasediments. At Koongarra subsequent reverse faulting has juxtaposed the lower Cahill Formation schists and Kombolgie Formation sandstone.

Owing to the isoclinal recumbent folding of metasedimentary units of the Cahill Formation, the typical rock sequence encountered at Koongarra is probably a tectono-stratigraphy (see Figure 3):–

Hanging Wall
- — muscovite-biotite-quartz-feldspar schist (at least 180 m thick)
- — garnet-muscovite-biotite-quartz schist (90–100 m thick)
- — sulphide-rich graphite-mica-quartz schist (±garnet) (about 25 m thick)
- — distinctive graphite-quartz-chlorite schist marker unit (5–8 m thick)

Mineralised Zone — quartz-chlorite schist (±illite, garnet, sillimanite, muscovite) (50 m thick)

Footwall
- — reverse fault breccia (5–7 m thick)
- — sandstone of the Kombolgie Formation

Polyphase deformation accompanied metamorphism of the original sediments, that were probably dolomite, shales and siltstones. Johnston[6] identified a D_2 event as responsible for the dominant S_2 foliation of the schist sequence, which at Koongarra dips at 55° to the south-east. The dominant structural feature, however, is the reverse fault system that dips at about 60° to the south-east, sub-parallel to the dominant S_2 foliation and lithological boundaries, just below the mineralised zone.

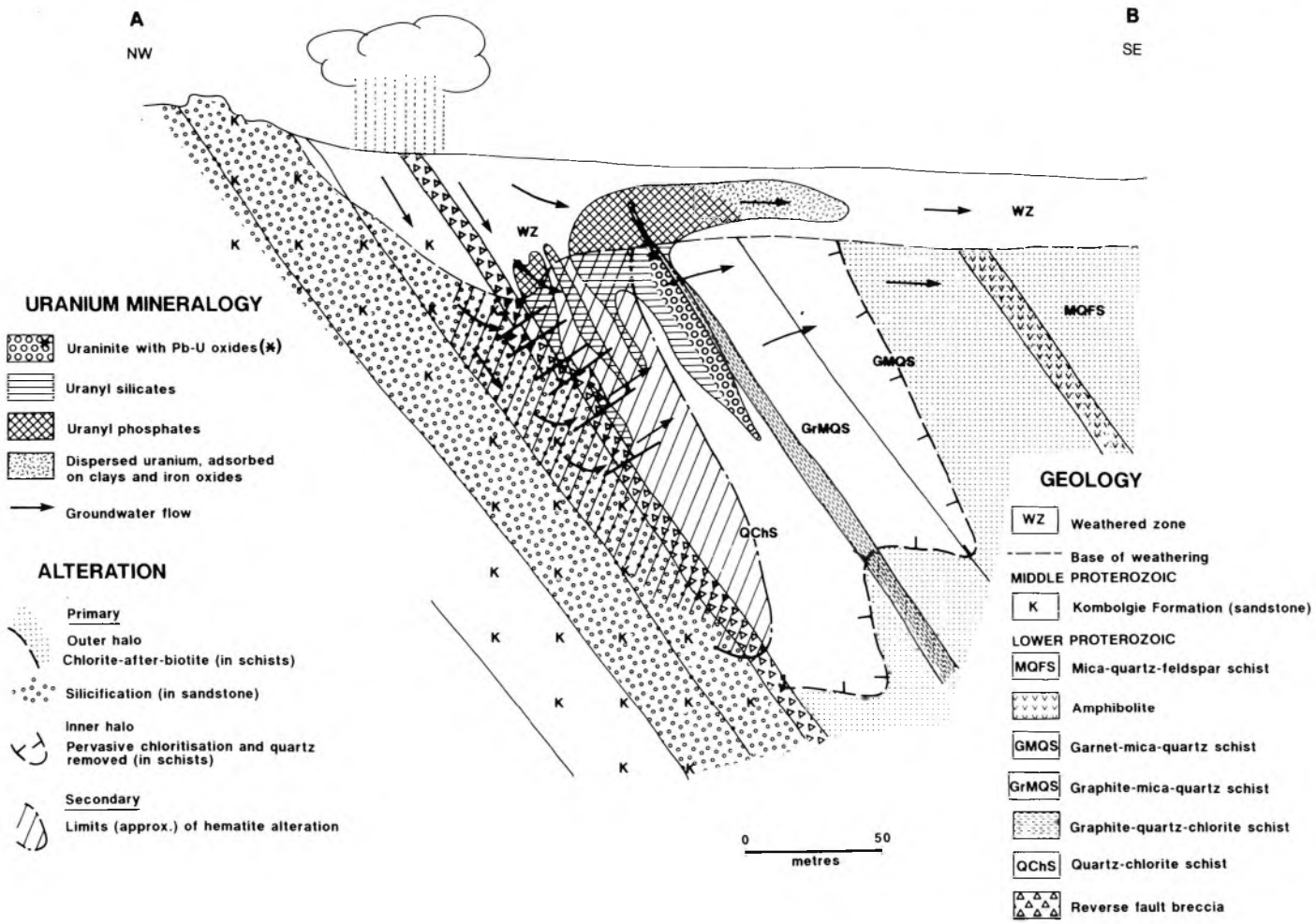

Figure 3. *Simplified cross section through the No. 1 orebody, Koongarra, showing geology, distribution of uranium minerals and alteration, and present groundwater flow.*

THE URANIUM DEPOSIT

There are two discrete uranium orebodies at Koongarra, separated by a 100 m wide barren zone (see Figure 2). The main (No. 1) orebody has a strike length of 450 m and persists to 100 m depth. Secondary uranium mineralisation is present in the weathered schists, from below the surficial sand cover to the base of weathering at depths varying between 25 and 30 m (see Figure 3). This secondary mineralisation has been derived from decomposition and leaching of the primary mineralised zone, and forms a tongue-like fan of ore-grade material dispersed down-slope for about 80 m to the south-east. The primary uranium mineralised zone in cross-section is a series of partially coalescing lenses, which together form an elongated wedge dipping at 55° to the south-east within the host quartz-chlorite schist unit, sub-parallel to the reverse fault. True widths average 30 m at the top of the primary mineralised zone but taper out at about 100 m below the surface and along strike.

Superimposed on the primary prograde metamorphic mineral assemblages of the host schist units is a distinct and extensive primary alteration halo associated, and cogenetic, with the uranium mineralisation (see Figure 3). This alteration extends for up to 1.5 km from the ore in a direction perpendicular to the host quartz-chlorite schist unit, because the mineralisation is essentially stratabound. The outer zone of the alteration halo is most extensively developed in the semi-pelitic schists, and is manifested by the pseudomorphous replacement of biotite by chlorite, rutile and quartz, and feldspar by sericite. Silicification has also occurred in fault planes and within the Kombolgie Formation sandstone beneath the mineralisation, particularly adjacent to the reverse fault. Association of this outer halo alteration with the mineralisation is demonstrated by the apparent symmetrical distribution of this alteration about the orebody. In the inner alteration zone, less than 50 m from ore, the metamorphic rock fabric is disrupted, and quartz is replaced by pervasive chlorite and phengitic mica, and garnet by chlorite. Uranium mineralisation is only present where this alteration has taken place.

The primary ore consists of uraninite veins and veinlets (1–10 mm thick) that cross-cut the S_2 foliation of the brecciated and hydrothermally altered quartz-chlorite schist host. Groups of uraninite veinlets are intimately intergrown

with chlorite, which forms the matrix to the host breccias. Small (10–100 μm) euhedral and subhedral uraninite grains are finely disseminated in the chloritic alteration adjacent to veins, but these grains may coalesce to form clusters, strings and massive uraninite. Coarse colloform and botryoidal uraninite masses and uraninite spherules with internal lacework textures have also been noted, but the bulk of the ore appears to be of the disseminated type, with thin (<0.5 mm) discontinuous wisps and streaks of uraninite, and continuous strings both parallel and discordant to the foliation (S_2), and parallel to phyllosilicate (001) cleavage planes.

Associated with the ore are minor volumes (up to 5%) of sulphides, which include galena and lesser chalcopyrite, bornite and pyrite, with rare grains of native gold, clausthalite (PbSe), gersdorffite-cobaltite (NiAsS-CoAsS) and mackinawite $(Fe, Ni)_{1.1}S$. Galena is the most abundant, commonly occurring as cubes (5–10 μm wide) disseminated in uraninite or gangue, and as stringers and veinlets particularly filling thin fractures within uraninite. Galena may also overgrow clausthalite, and replace pyrite and chalcopyrite. Chlorite, predominantly magnesium chlorite, is the principal gangue, and its intimate association with the uraninite indicates that the two minerals formed together.

Oxidation and alteration of uraninite within the primary ore zone has produced a variety of secondary uranium minerals, principally uranyl silicates.[7] Uraninite veins, even veins over 1 cm wide, have been completely altered *in situ*. Within the primary ore zone this *in situ* replacement of uraninite is most pronounced immediately above the reverse fault breccia, and this alteration and oxidation diminish upwards stratigraphically. It is accompanied by hematite staining of the schists, the more intense hematite alteration in and near the reverse fault breccia being due to hematite replacement of chlorite. The secondary mineralisation of the dispersion fan in the weathered schist above the No. 1 orebody is characterised by uranyl phosphates found exclusively in the 'tail' of the fan. Away from the tail uranium is dispersed in the weathered schists and adsorbed onto clays and iron oxides.

The 'age' of the uranium mineralisation is problematical. The mineralisation, however, must post-date both the Kombolgie Formation sandstone and the Koongarra reverse fault, since it occupies the breccia zones generated by the post-Kombolgie reverse faulting. The pattern of alteration which is intimately associated with the ore also crosses the reverse fault into the Kombolgie sandstone beneath the ore zone, so this again implies that the ore was formed after the reverse fault and therefore is younger than both the Kombolgie sandstone and the reverse fault. Because of these geological constraints, Page *et al.*[8] suggested the mineralisation was younger than 1600–1688 Ma because of their determination of the timing of the Kombolgie Formation deposition to that period. Sm-Nd isotopic data obtained on Koongarra uraninites[9,10] appears to narrow down the timing of mineralisation to 1550–1650 Ma. It is unclear as to when deep groundwater circulation began to cause oxidation and alteration of the primary uraninite ore at depth, but Airey *et al.*[11] suggest that the weathering of the primary ore to produce the secondary dispersion fan in the weathered schists above the No. 1 orebody seems to have begun 'only' in the last 1–3 Ma.

EVIDENCE OF AN OPEN SYSTEM

There are five main lines of independent evidence that the mineral-rock systems at Koongarra have been open to diffusion and migration of U, Th and daughter isotopes including Pb. Such behaviour of these isotopes has crucial implications to all attempts to 'date' the Koongarra uranium ore using the U-Th-Pb isotopic systems.

(1) Ore Textures

Mineralogical and textural studies of the ore under both optical and scanning electron microscopes[12,13] indicate that there have been as many as three remobilisations of the uranium during the history of the ore. Pb has likewise been mobile. That is, both the primary U and Pb minerals, uraninite and galena respectively, have been dissolved and redeposited/recrystallised, often some distance away from their original locations. This is shown diagrammatically in Figure 4 as several generations of uraninite and galena.

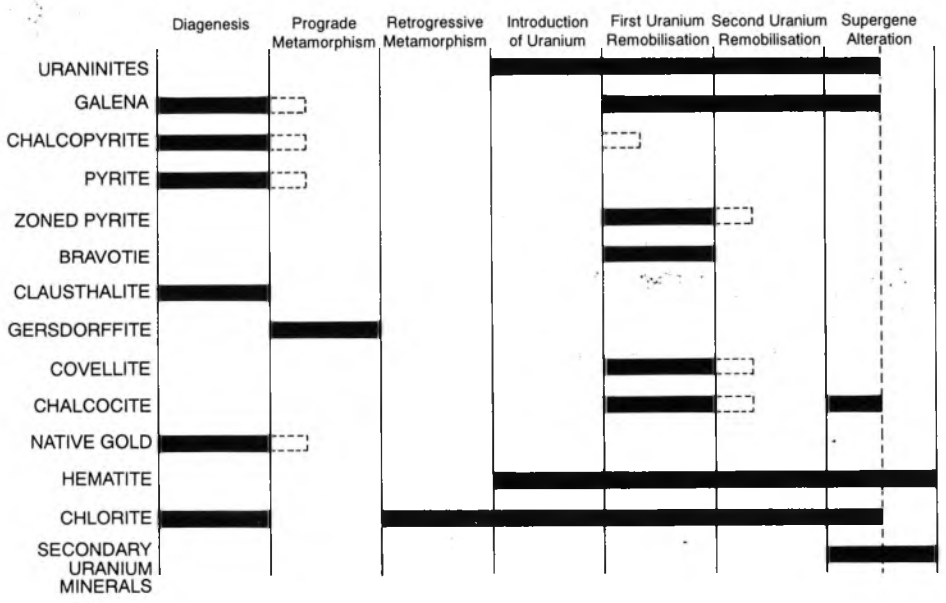

Figure 4. *Paragenesis diagram showing the stages of formation and development of the minerals comprising the Koongarra uranium deposit.*

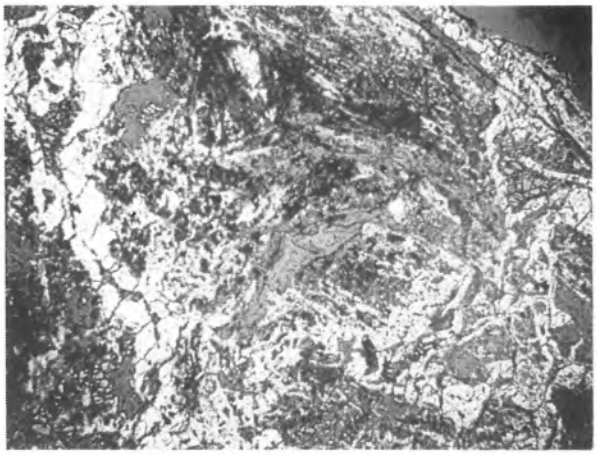

Figure 5. *Remobilisation and redeposition of uraninite (white mineral). Photomicrograph shows uraninite veins (left and right) partially destroyed by dissolution of uranium which has been redeposited as scattered veinlets and shapeless masses of a new generation of uraninite (middle). (Magnification 10X).*

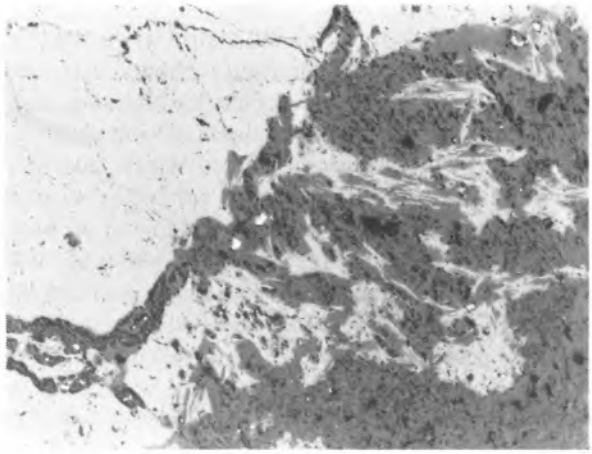

Figure 6. *Uraninite (light grey) has been dissolved and redeposited as thin veinlets and shapeless masses within a chlorite (dark grey) matrix which is also replacing the main uraninite grain. (Magnification 120X).*

Figure 7. *Two generations of uraninite grains (lighter grey), and more oxidised supergene veins and patches (darker grey). The small scattered white grains are galena. (Magnification 200X).*

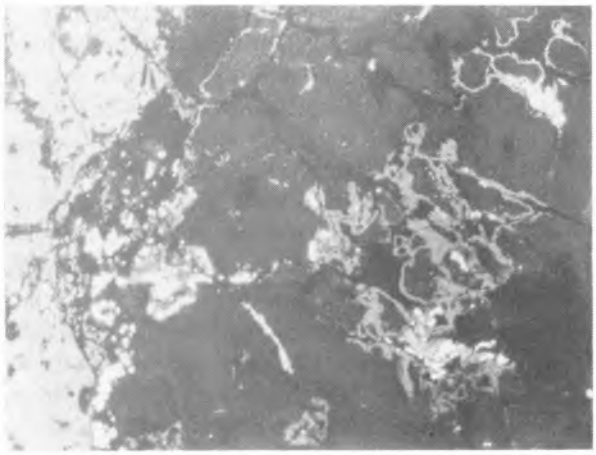

Figure 8. *Two generations of uraninite grains (white, left of photomicrograph) and later thin supergene encrustations (mid grey) around quartz grains (dark grey). The very bright mineral (right) is galena which has similarly been dissolved and redeposited. (Magnification 200X).*

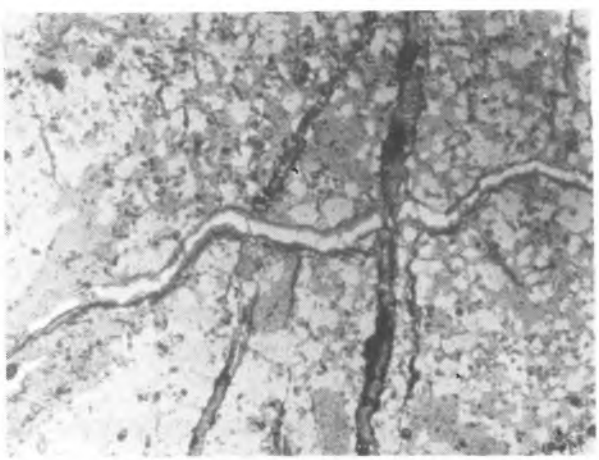

Figure 9. *Remobilised uraninite (light grey) deposited as scattered grains with a chlorite (dark grey) matrix. A remobilised galena vein (white-grey) cuts across the uraninite-chlorite association. (Magnification 50X).*

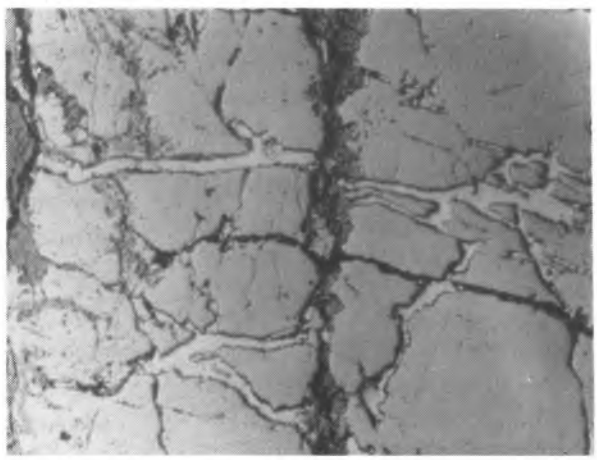

Figure 10. *An enlarged view of uraninite (dark grey) sub-grains within a larger vein. Galena (light grey) veinlets which both cross-cut and separate the uraninite sub-grains. The Pb in the galena is supposed to have migrated from the uraninite where it was supposedly produced by radioactive decay. (Magnification 50X).*

	PS 17860/1								PS 17863/4		
	1	2	3	4	5	6	7	8	1	2	3
UO_2	89.17	89.43	89.65	89.86	90.70	91.14	91.27	91.29	92.20	89.77	88.91
PbO	7.67	7.22	6.67	6.14	5.93	5.31	4.92	4.57	5.70	5.65	4.66
CaO	1.64	1.77	1.73	1.82	1.83	1.79	1.80	2.13	0.38	0.38	0.27
SiO_2	0.39	0.42	0.43	0.46	0.53	0.57	0.56	0.50	0.24	1.00	2.34
ΣFe (FeO)	0.45	0.44	0.46	0.49	0.44	0.46	0.45	0.46	l.d.	0.11	0.46
MnO	–	–	–	–	–	–	–	–	–	–	–
MgO	l.d.	0.11	l.d.	l.d.	0.11	0.11	l.d.	0.12	0.39	0.94	1.86
P_2O_5	0.21	0.21	0.19	0.16	0.23	0.18	0.23	0.30	0.13	0.17	0.13
Total	99.53	99.60	99.13	98.93	99.77	99.56	99.23	99.37	99.04	98.02	98.91

	PS 17862/3									
	1	2	3	4	5	6	7	8	9	10
UO_2	85.58	86.35	86.45	86.96	87.26	88.04	88.48	89.63	89.81	86.64
PbO	11.29	10.69	10.25	9.86	9.24	8.48	7.93	6.73	6.27	6.79
CaO	1.68	1.51	1.56	1.58	1.64	1.74	1.86	1.83	2.09	1.81
SiO_2	0.50	0.41	0.46	0.47	0.45	0.46	0.53	0.60	0.63	0.78
ΣFe (FeO)	0.56	0.48	0.52	0.49	0.50	0.46	0.45	0.47	0.58	2.09
MnO	0.38	0.35	0.38	0.36	0.36	0.40	0.36	0.30	0.35	0.29
MgO	0.24	0.17	0.13	0.13	0.12	0.10	0.15	0.15	l.d.	0.18
P_2O_5	0.16	0.14	0.17	0.13	0.14	0.17	0.12	0.17	0.19	1.14
Total	100.39	100.10	99.92	99.98	99.71	99.85	99.80	99.88	99.92	99.72

	PS 17865/6										
	1	2	3	4	5	6	7	8	9	10	11
UO_2	85.40	85.97	86.47	86.46	87.07	87.79	88.53	89.14	89.30	90.24	90.52
PbO	12.22	11.21	10.73	10.14	9.43	8.79	8.31	7.83	7.20	6.24	5.93
CaO	1.17	1.45	1.33	1.90	1.79	1.79	1.81	1.99	2.02	2.01	1.95
SiO_2	0.33	0.36	0.36	0.49	0.51	0.47	0.52	0.49	0.43	0.58	0.48
ΣFe (FeO)	0.37	0.39	0.36	0.48	0.53	0.49	0.51	0.47	0.56	0.47	0.45
MnO	0.27	0.31	0.31	0.34	0.37	0.32	0.30	0.35	0.34	0.38	0.35
MgO	0.34	0.26	0.28	0.23	0.16	0.18	0.18	0.13	0.28	0.13	0.18
P_2O_5	0.13	0.12	0.15	0.15	0.16	0.14	0.15	0.14	0.16	l.d.	0.16
Total	100.23	100.07	99.63	100.19	99.89	99.97	100.31	100.54	100.29	100.05	100.02

	PS 17867/8			PS 17868/9					
	1	2	3	1	2	3	4	5	6
UO_2	84.81	85.13	86.24	89.03	89.54	85.12	86.77	81.34	82.41
PbO	10.49	9.11	8.30	5.19	5.14	8.34	9.36	11.46	10.29
CaO	1.37	1.89	1.86	2.70	3.15	4.68	2.17	3.77	4.06
SiO_2	2.38	1.35	1.54	1.20	0.85	0.83	0.70	1.20	0.99
ΣFe (FeO)	0.33	0.44	0.34	0.43	0.52	l.d.	0.53	l.d.	l.d.
MnO	–	–	–	–	–	–	–	–	–
MgO	0.54	0.17	0.20	0.10	l.d.	0.19	0.11	0.12	0.16
P_2O_5	l.d.	l.d.	0.14	0.14	0.11	0.56	l.d.	0.43	0.50
Total	99.92	98.09	98.62	98.79	99.31	99.72	99.64	98.32	98.41

[– denotes not measured; l.d. denotes less than detection limits]

Table 1. *Analyses of some representative Koongarra uraninites.*

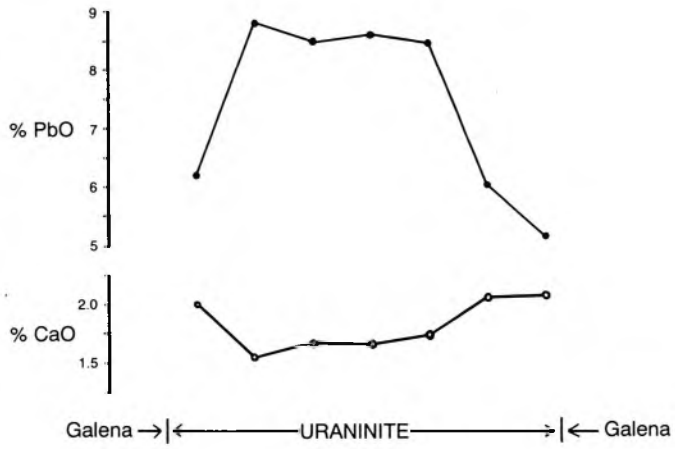

Figure 11. *Compositional traverse across a uraninite grain similar to those in Figure 10.*

Figures 5–10 illustrate examples of the ore textures under the microscopes, the accompanying descriptions indicating how the textures have been interpreted.

(2) Mineral Chemistry

Uraninite compositions in the ore are never uniform. Electron microprobe analyses of uraninite grains and veins,[14] that is, micro-analyses of volumes of uraninite between 5 and 10 μm in diameter (see Table 1), reveal that uraninite compositions, particularly U, Pb and Ca contents, vary not only from grain to grain within any one sample regardless of which generation of uraninite it is, but even at the microscopic level within uraninite grains themselves. Figure 11 illustrates how Pb and Ca have both substituted for U in the UO_2 cubic lattice in varying amounts across the uraninite veins and grains.

(3) Supergene Alteration

As has already been briefly noted, supergene alteration (principally oxidation) of uraninite has not only occurred where the zone of surficial weathering has intersected the top of the No. 1 orebody, but at depth within the primary ore. Uraninite grains and veins have been replaced by colourful secondary uranium minerals (see Table 2), their occurrence and compositions depending on the chemistries of the immediate rock/mineral environments and the circulating ground waters (see Figures 3 and 12). The net result has been the complete destruction of the uraninite in what was the top of the No. 1 orebody, with its replacement (sometimes *in situ*) by uranyl silicate or uranyl phosphate minerals (usually the latter), and the dispersion of the rest of the U over distances of up to 50 m or more down-slope by

Uranium — Lead Oxides	
Curite	$2PbO \cdot 5UO_3 \cdot 4H_2O$
Fourmarierite	$PbO \cdot 4UO_3 \cdot 4H_2O$
Vandendriesscheite	$PbO \cdot 7UO_3 \cdot 12H_2O$
Uranyl Silicates	
Kasolite	$Pb(UO_2)SiO_4 \cdot H_2O$
Sklodowskite	$Mg(UO_2)_2Si_2O_7 \cdot 6H_2O$
Uranophane	$Ca(UO_2)_2Si_2O_7 \cdot 6H_2O$
Uranyl Phosphates	
Saleeite	$Mg(UO_2)_2(PO_4)_2 \cdot 8\text{-}10H_2O$
Sabugalite	$HAl(UO_2)_4(PO_4)_4 \cdot 16H_2O$
Metatorbernite	$Cu(UO_2)_2(PO_4)_4 \cdot 8H_2O$
Torbernite	$Cu(UO_2)_2(PO_4)_2 \cdot 8\text{-}12H_2O$
Renardite	$Pb(UO_2)_4(PO_4)_2(OH)_4 \cdot 7H_2O$
Dewindtite	$Pb(UO_2)_2(PO_4)_2 \cdot 3H_2O$
Uranyl Sulphate	
Johannite	$Cu(UO_2)_2(SO_4)_2(OH)_2 \cdot 6H_2O$
Uranyl Vanadates	
Carnotite — Tyuyamunite	$K_2(UO_2)_2(VO_4)_2 \cdot 3H_2O$ — $Ca(UO_2)_2(VO_4)_2 \cdot 5\text{-}8H_2O$

Table 2. *The secondary uranium minerals at Koongarra.*

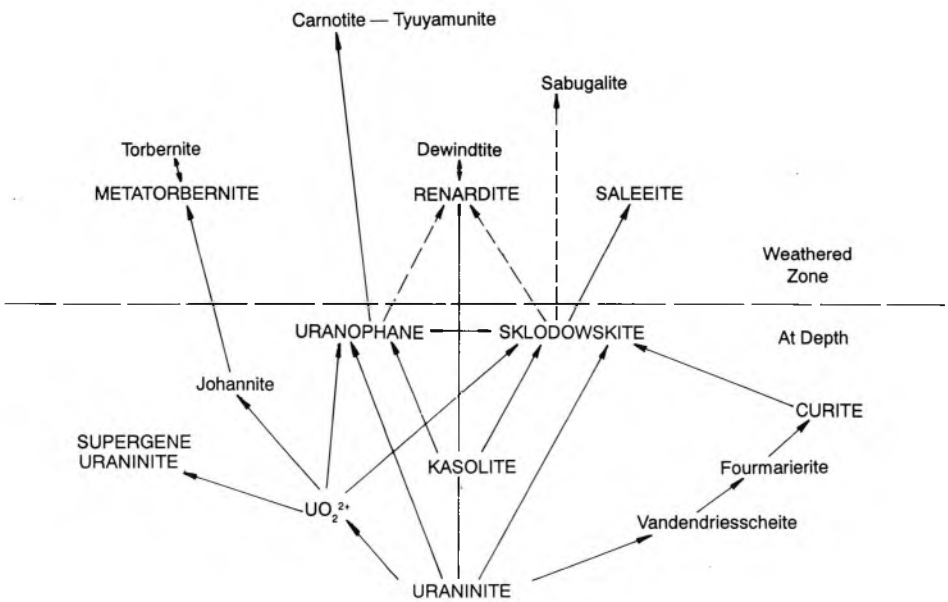

Figure 12. *Schematic diagram showing the paths of secondary uranium mineral formation from uraninite in the Koongarra uranium deposit.*

Figure 13. *Kasolite (white) and uranophane (grey) replacing a former uraninite vein. Note that the former vein shape, even the sub-grains, have essentially been preserved. (SEM magnification 210X; scale bar 50 microns.)*

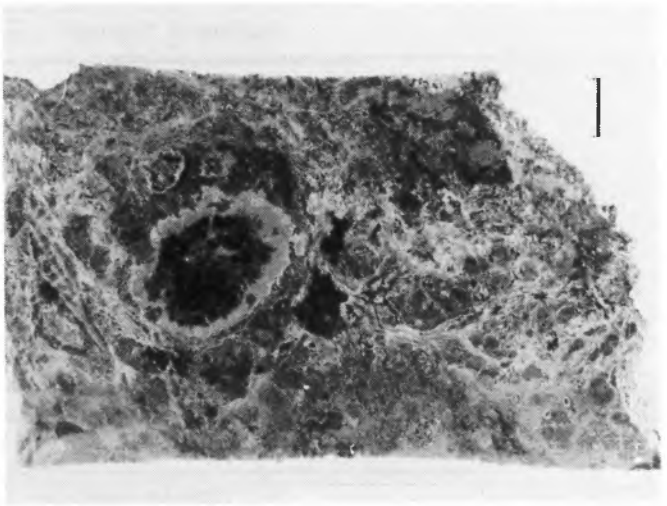

Figure 14. *Gobular uraninite mass (black shape just to the left of centre) being altered marginally to sklodowskite (grey concentric sheath). (Magnification 2X; scale bar 3 mm.)*

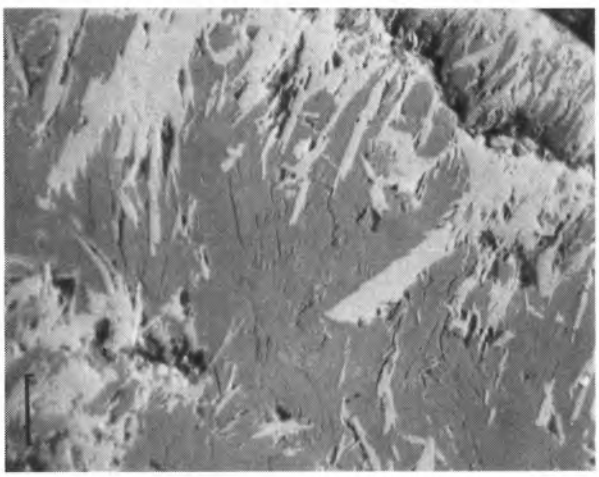

Figure 15. *Kasolite (light grey) and sklodowskite (dark grey) replacing a former uraninite vein. (SEM magnification 210X.)*

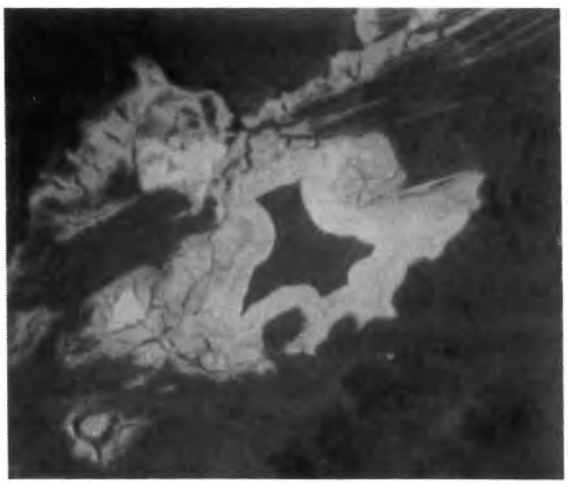

Figure 16. *Supergene colloform banded uraninite (grey) deposited in what was originally a void. The banding is produced by a time sequence of uraninite deposition. (SEM magnification 840X.)*

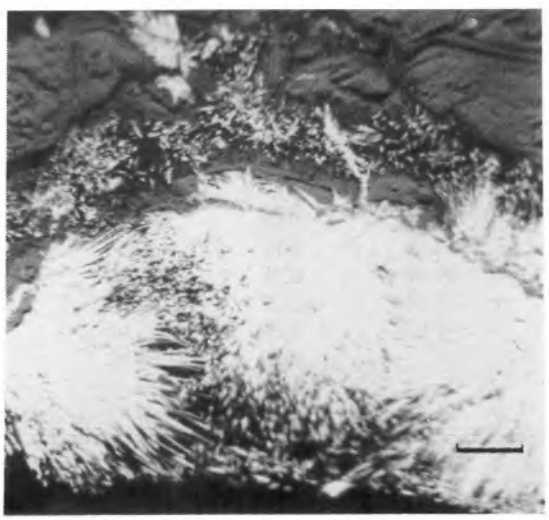

Figure 17. *A sklodowskite (white) vein composed of radiating aggregates of needle-shaped crystals. (SEM magnification 220X; scale bar 50 microns.)*

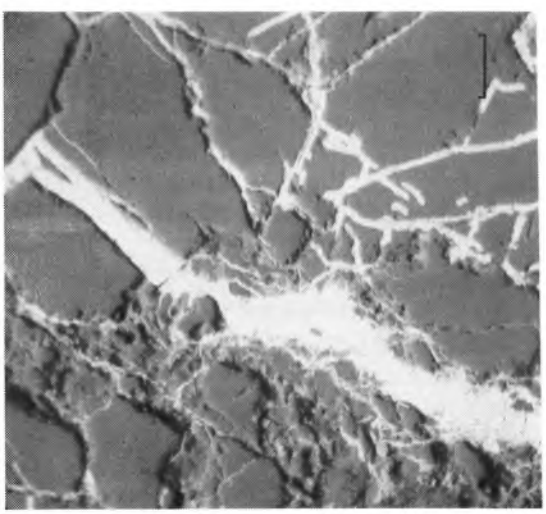

Figure 18. *Uranophane (white) veinlets deposited between quartz (grey) grain boundaries. (SEM magnification 220X; scale bar 50 microns.)*

PS 17867/8: Uraninite → Uranophane – Sklodowskite						
	1	2	3	4	5	6
UO_2	84.81	85.13	86.24	76.74	69.58	66.45
PbO	10.49	9.11	8.30	8.99	1.05	0.15
CaO	1.37	1.89	1.86	2.89	4.89	3.86
SiO_2	2.38	1.35	1.54	5.53	12.06	14.83
ΣFe (FeO)	0.33	0.44	0.34	0.29	0.70	l.d.
MgO	0.54	0.17	0.20	0.75	1.16	4.76
Al_2O_3	0.11	l.d.	l.d.	0.75	l.d.	0.31
P_2O_5	l.d.	l.d.	0.14	0.36	0.35	0.34
V_2O_3	l.d.	l.d.	l.d.	0.24	0.31	l.d.
Total	100.03	98.09	98.62	96.54	90.10	90.70

CAS 195: Uraninite → Uranophane – Sklodowskite									
	1	2	3	4	5	6	7	8	9
UO_2	82.18	85.49	86.22	88.27	90.53	63.74	68.76	66.50	66.44
PbO	11.55	9.34	7.93	6.39	4.65	9.83	4.48	3.55	1.60
CaO	3.08	2.80	3.15	3.13	3.06	2.34	2.98	2.77	2.86
SiO_2	1.48	1.66	1.64	1.50	1.14	11.58	9.95	12.00	12.30
ΣFe (FeO)	0.80	0.40	0.88	0.39	0.41	0.87	0.20	0.23	l.d.
MgO	l.d.	l.d.	l.d.	l.d.	l.d.	0.39	0.19	0.20	1.13
Al_2O_3	–	–	–	–	–	–	–	–	–
P_2O_5	l.d.	0.13	l.d.	l.d.	l.d.	2.38	2.15	2.86	2.11
V_2O_3	–	–	–	–	–	–	–	–	–
Total	99.09	99.82	99.82	99.68	99.79	91.13	88.71	88.11	86.44

[– denotes not measured; l.d. denotes less than detection limits]

Table 3. *Analyses of alteration sequences of uraninites to uranyl silicates at Koongarra.*

ground waters in the weathered zone. Additionally, at the same time there has been yet another remobilisation of both U and Pb in the primary ore zones, with *in situ* replacement of uraninite (see Figures 13–15) and deposition of supergene uraninite (see Figure 16) and the uranyl silicate minerals sklodowskite and uranophane (see Figures 17 and 18) from the U in solution from circulating ground waters (see Figure 3 again).[15] Electron microprobe analyses (see Table 3) show that the U and Pb contents have decreased as uraninites were altered to uranyl silicates, while the iron and manganese oxides lining fractures in the host rocks have absorbed the U and Pb that had been dissolved during the oxidation of the uraninites and migrated in the circulating ground waters (see Table 4).

(4) Uranium/Daughter Disequilibrium

There are two methods of measuring the grade of a uranium ore sample:–

(i) by assaying for U directly using standard chemical or related techniques, and

	CAS 165	CAS 114/1	CAS 114/2	CAS 95/1	CAS 95/2	CAS 95/3
UO_2	2.81	1.63	1.05	0.36	2.83	1.91
PbO	12.42	4.41	0.30	5.03	8.16	3.34
CaO	0.20	0.09	l.d.	0.04	0.15	0.12
SiO_2	2.49	3.11	6.28	2.87	2.54	3.20
ΣFe (FeO)	5.50	8.71	81.46	0.47	11.09	58.16
MnO_2	77.48	80.35	1.96	88.52	73.53	27.70
MgO	0.12	0.37	2.09	0.29	0.52	0.22
Al_2O_3	0.15	1.23	–	2.70	0.82	1.75
P_2O_5	0.33	l.d.	–	–	l.d.	l.d.
V_2O_3	l.d.	–	–	0.31	0.65	0.26
Total	101.50	99.90	93.14	100.59	100.29	96.66

[– denotes not measured; l.d. denotes less than detection limits]

Table 4. *Analyses of iron and manganese oxides in fractures in the Koongarra primary ore.*

No.	Group Description	No. of Samples	Average U_3O_8(%)	Average Ratio	σ^a
No. 1 Orebody					
1	Weathered zone	13	0.275	0.914	0.160
2	Host wall rocks	19	0.025	0.792	0.151
3	Massive ore	11	8.074	0.959	0.069
4	Intermediate between No. 1 and 2 orebodies	2	0.171	0.971	0.132
No. 2 Orebody					
5	Massive ore	9	1.608	0.925	0.102
Total number of samples		54	Mean =	0.884	0.127

[a] Standard deviations of average ratio

Table 5. *Summary of disequilibrium patterns in the Koongarra orebodies.*

(ii) by measuring the radioactivity given off by the ore sample, the quantity of such radioactivity being directly related, and proportional, to the U content.

However, because the radioactivity measured is actually the gamma radiation given off by the daughter element bismuth-214 (^{214}Bi) far down the ^{238}U decay chain, any addition or removal of daughter elements between ^{238}U and ^{214}Bi will result in a discrepancy between the above two measurements of the U content of the ore sample. To assess this possibility the two measurements are compared:–

$$\text{Disequilibrium Ratio} = \frac{\text{U content (chemical)}}{\text{U content (radioactive)}}$$

Three possibilities arise:–

(a) Ratio = 1. The ore sample is said to be in equilibrium since the two measurements agree, implying that the U and its daughter elements are in equilibrium; neither have apparently migrated.

(b) Ratio>1. The ore sample is said to be in disequilibrium, and since the U content is greater than the daughter element content either U has been added to the sample or daughter elements removed.

(c) Ratio<1. Again the ore sample is said to be in disequilibrium, but now the U content is less than the daughter element content implying either U removal or daughter element addition to the sample.

Measurements on ore samples from Koongarra indicate that the ore is in overall disequilibrium (Table 5 and Figure 19).[16] High resolution gamma-ray spectroscopy was then used to determine which daughter elements of ^{238}U have been mobilised.[17] These investigations showed that even though the high grade uraninite (massive) ore is near equilibrium, radium–226 (^{226}Ra) and radon–222 (^{222}Rn), a gas, have migrated from the ore into the surrounding host rocks, the ore being generally depleted in ^{226} Ra and ^{222}Rn, and the immediate host rocks being relatively enriched in those two isotopes. As expected, the weathered top of the No. 1 orebody is depleted in U, whereas down-slope in the weathered zone the weathered host rocks are relatively enriched in U, having been precipitated from the circulating ground waters that had dissolved it from the orebody. Figure 20 schematically

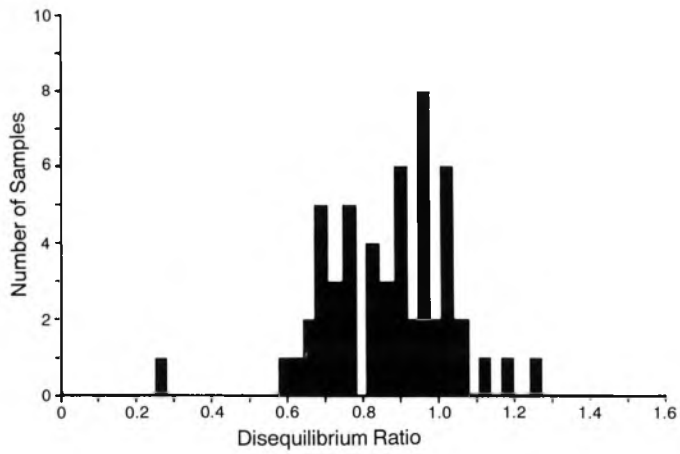

Figure 19. *Frequency histogram of disequilibrium ratios measured on Koongarra ore and host rock samples.*

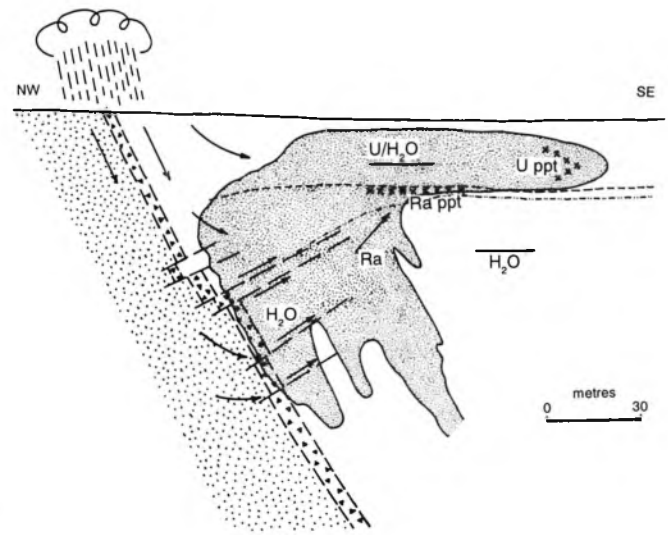

Figure 20. *Uranium (U) and radium (Ra) migration and precipitation (ppt) caused by present-day groundwater circulation and chemistry.*

Sample No.	Concentration (Wt %)			Atomic Ratios			Ages			Lead Isotope Ratios		
	%U	%Pb	%Th	N206/N238	N207/N235	N207/N206	t206 m.y.	t207 m.y.	t207/206 m.y.	206/204	207/204	208/204
J804/1	62.38	8.07	0.30	0.142	1.312	0.0673	861	862	864	21330.	1450.	7.10
J804/b	38.21	4.45	0.28	0.126	1.264	0.0727	774	841	1025	9875.	731.9	34.84
J801	55.07	3.64	0.34	0.071	0.810	0.0826	447	610	1282	16870.	1408.	54.20
J807	44.08	5.35	0.33	0.130	1.259	0.0703	796	838	954	12920.	921.9	35.49
J809	52.61	5.45	0.39	0.114	1.061	0.0679	699	744	882	105800.	7200.	62.64
Common lead correction **Mt Isa lead**										16.11	15.61	36.72

Table 6. *U-Th-Pb concentrations and isotopic compositions of Koongarra uraninites.*

illustrates these movements of isotopes caused by the present day circulation of the ground waters.

(5) Groundwater and Soil Geochemistry

Because of the tropical, monsoonal climate, the ground waters in the Koongarra area are fast moving, annually recharged and low in salinity, the water table rising and falling by as much as 10 m between the wet and the dry seasons. However, U is dissolved by the ground waters from the mineralised aquifer rocks, the level of dissolved U depending on the prevailing pH, Eh, salinity and degree of adsorption. A survey of the chemistry of the ground waters in open drill holes in and near the Koongarra orebodies revealed that a hydrogeochemical halo exists in and around the ore zones reflecting the alteration chemistry of the host rocks and ore, with U levels up to 4100 μg/l.[18] Such measurements confirm the other observations already cited that indicate U is being dissolved from the ore minerals by present day circulating ground waters, dispersed and partly redeposited. Furthermore, the ground waters are also dispersing U-Th decay products such as helium (He) from the ore zone, with measured levels up to 14.2 μl/l.[19]

It is hardly surprising, therefore, that the soils overlying the ore zones and the immediate areas of host rocks carry anomalous U concentrations compared to background levels.[20] That the ground waters have been responsible for dispersing U (and Pb) into the surrounding soils is also clearly demonstrated by analyses down through the soil profile. Furthermore, Dickson *et al.*[21,22] found the Pb isotopic signature of the U ore in the soils above the No. 2 orebody, which is concealed by about 40 m of barren overburden, and in the soils to the south of the No. 1 orebody within the hydrogeochemical halo.

Sample No.	206/204	207/204	208/204
J801	10290.	1016.	55.81
J803	41240.	3258.	143.9
J804	11530.	883.	8.539
J809	10540	1261.	47.41
J820	4824.	709.2	35.15
J821	3399.	461.0	43.24

Table 7. *Isotopic compositions of Koongarra galenas.*

U-TH-PB DATA

'Dating' of the Primary Ore

Hills and Richards[23,24] isotopically analysed individual grains of uraninite and galena that had been hand-picked from drill core (see Tables 6 and 7). Only one of the five

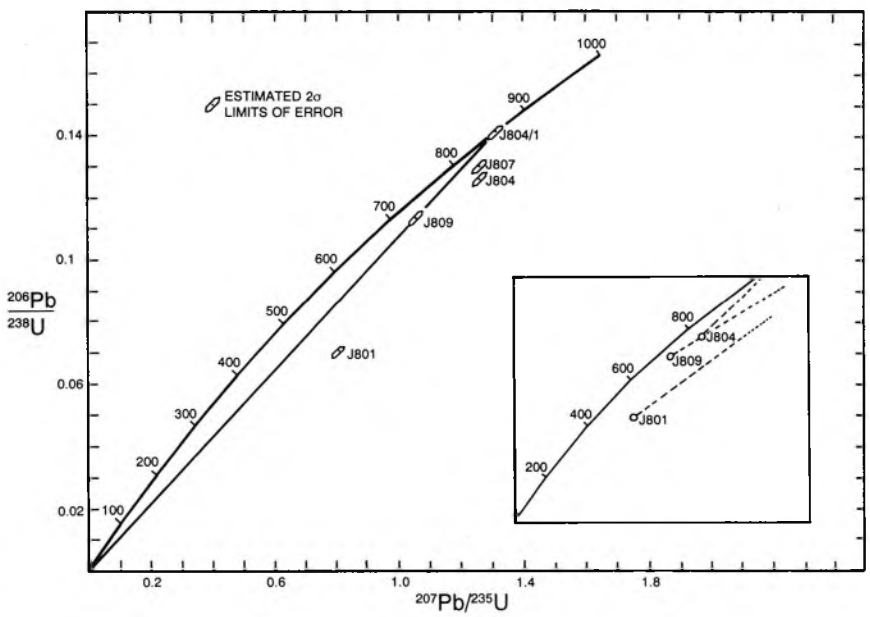

Figure 21. *Conventional $^{206}Pb/^{238}U$ vs $^{207}Pb/^{235}U$ concordia diagram of uraninites from Koongarra. The insert shows the hypothetical directional shift in uraninite data points supposedly explained by contamination from associated galena.*

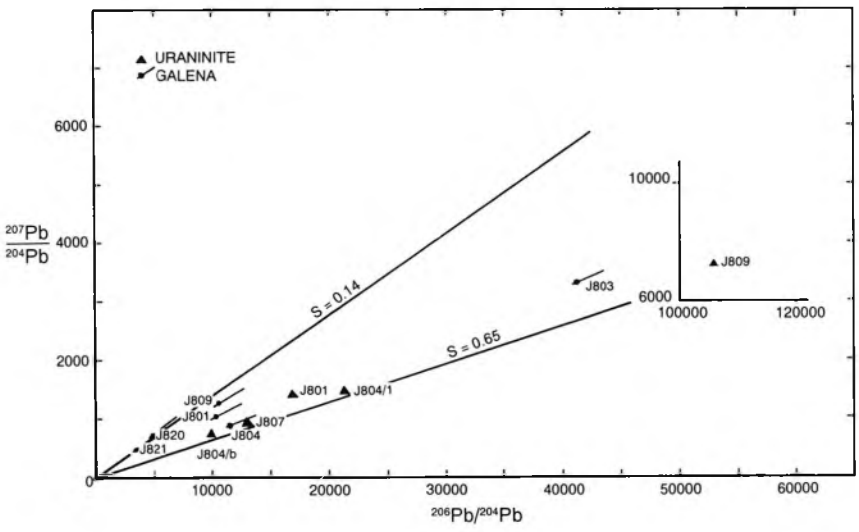

Figure 22. *Conventional $^{207}Pb/^{204}Pb$ vs $^{206}Pb/^{204}Pb$ plot of galenas and uraninites from Koongarra. Limiting fields of anomalous-lead lines corresponding to 'ages' of 1800 Ma and 860 Ma are also shown.*

uraninite samples gave a near-concordant 'age' of 862 Ma, that is, the sample plotted almost on the standard concordia curve, and Hills and Richards[25] interpreted this as recording fresh formation of Pb-free uraninite at 870 Ma (see Figure 21). The other four uraninite samples all lay well below concordia and did not conform to any regular linear array. Hills and Richards were left with two possible interpretations. On the one hand, preferential loss of the intermediate daughter products of ^{238}U (that is, escape of radon, a gas) would cause vertical displacement of points below an episodic-loss line, but this would only produce a significant Pb isotopic effect if the loss had persisted for a very long proportion of the life of the uraninite (which is incidentally not only feasible but likely). Alternatively, they suggested that contamination by small amounts of an older (pre-900 Ma) Pb could cause such a pattern as on their concordia plot, to which they added mixing lines that they postulated arose from the restoration to each uraninite sample of the galena which separated from it (see Figure 21 again).

This of course assumes that the Pb in the galenas was also derived predominantly from U decay. They plotted their Pb ratios in all their uraninite samples on a standard $^{207}Pb/^{206}Pb$ diagram, and contended that the pattern of data points did not conform to a simple age interpretation (see Figure 22). Instead, they contended that the scatter of points could be contained between two lines radiating from the diagram's origin, lines that essentially represented isochrons for uraninites and galenas from the Ranger and Nabarlek uranium deposits, similar orebodies in the same geological region. From the positions of the Koongarra uraninites and galenas on these diagrams they claimed that the galenas contained left-over radiogenic Pb from earlier uraninites as old as 1700–1800 Ma (the 'age' of the Ranger uranium mineralisation), these earlier uraninites being obliterated by the U having remobilised at 870 Ma, the 'age' of the lone Pb-free uraninite sample.

In a separate study Carr and Dean[26] isotopically analysed unweathered whole-rock samples from the Koongarra primary ore zone (see Table 8). These were samples of drill core that had been crushed. Their isotopic data on four samples were plotted on a U-Pb isochron diagram and indicated a non-systematic relationship between the ^{238}U parent and the ^{206}Pb daughter. In other words, the quantities of ^{206}Pb could not simply be accounted for by radioactive decay of ^{238}U, implying open system behaviour. They also plotted their four results on a standard $^{207}Pb/^{206}Pb$ isochron diagram (see Figure 23) and found that these samples fell on a poorly defined linear array whose apparent age they did not quantify.

'Dating' of Weathered Rocks and Soils

Carr and Dean[27] also isotopically analysed a further nine whole-rock samples from the weathered schist zone at Koongarra (see Table 8). Some of these samples were again crushed drill core, but the majority were crushed percussion drill chips. When their isotopic data were plotted on a U-Pb isochron diagram, six of the nine samples plotted close to the reference 1000 Ma isochron, while the other three were

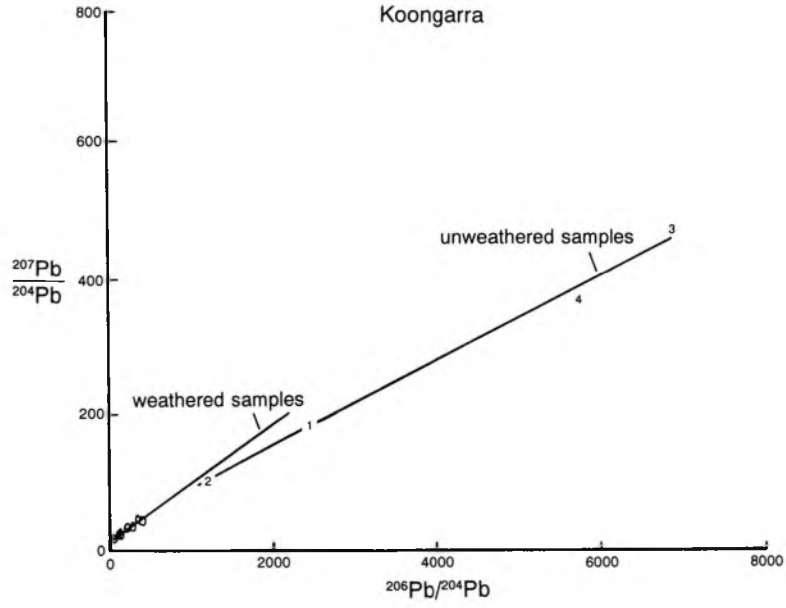

Figure 23. *Conventional $^{207}Pb/^{204}Pb$ vs $^{206}Pb/^{204}Pb$ plot of the weathered and unweathered whole-rock samples from Koongarra. The weathered and unweathered samples fall on separate 'isochrons'.*

Sample	$\frac{208Pb}{206Pb}$	$\frac{207Pb}{206Pb}$	$\frac{206Pb}{204Pb}$	$\frac{207Pb}{204Pb}$	$\frac{208Pb}{204Pb}$	Pb (ppm)	U (ppm)
Primary Ore							
1	0.0233	0.0752	2438.350	183.370	56.708	80	590.0
2	0.0682	0.0908	1162.990	105.594	79.351		168.0
3	0.0110	0.0692	6845.720	473.718	75.415	112	154.0
4	0.0346	0.0649	5719.990	371.474	198.191	19	17.0
Weathered Zone Ore							
5	0.1785	0.1192	387.664	46.210	69.205	5	413.0
6	0.3804	0.2028	124.773	25.310	47.465	5	861.0
7	0.5029	0.2790	72.814	20.315	36.616	50	
8	0.9277	0.4118	44.155	18.184	40.964	10	
9	0.1608	0.1403	248.526	34.859	39.963	30	
10	0.1650	0.1420	241.053	34.225	39.772	30	
11	1.0477	0.3534	55.190	19.502	57.822	3	
12	0.1213	0.1252	363.622	45.537	44.119	58	
13	0.1233	0.1250	357.688	44.709	44.106	10	

Table 8. *Results of Pb isotopic, U concentration and Pb concentration analyses for Koongarra whole-rock samples.*

widely scattered (see Figure 24). However, on the $^{207}Pb/^{206}Pb$ diagram all nine weathered rock samples plotted on a linear array which gave an apparent isochron 'age' of 1270 ±50Ma (see Figures 23 and 25).

In unrelated investigations, Dickson *et al.*[28,29] collected soil samples from above the mineralisation at Koongarra and from surrounding areas, and these were analysed for Pb isotopes to see if there was any Pb isotopic dispersion halo around the mineralisation sufficiently large enough to warrant the use of Pb isotopic analyses of soils as an exploration technique to find new uranium orebodies. The technique did in fact work, Pb isotopic traces of the deeply buried No. 2 orebody mineralisation being found in the soils above, as mentioned earlier. This mineralisation, 40 m below the surface, is blind to other detection techniques.

Dickson *et al.*[30] found that all 113 soil samples from their two studies were highly correlated (r = 0.99986) on a standard $^{207}Pb/^{206}Pb$ diagram, yielding an apparent (false) isochron representing an 'age' of 1445 ±20 Ma for the samples (see Figure 26). However, most of the soil samples consisted of detritus eroded from the Middle Proterozoic Kombolgie sandstone, so because the samples from near the mineralisation gave a radiogenic Pb signature Dickson *et al.* interpreted the false 'isochron' as being due to mixing of radiogenic Pb from the uranium mineralisation with the 'common' Pb from the sandstone.

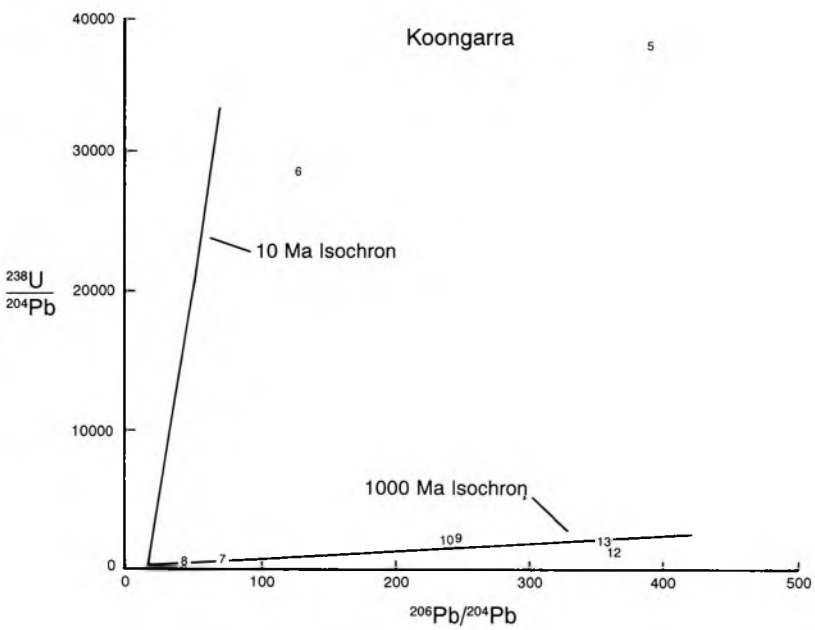

Figure 24. *A U-Pb ($^{238}U/^{204}Pb$ vs $^{206}Pb/^{204}Pb$) isochron diagram with the weathered whole-rock samples plotted on it. Most fall on the 1000 Ma reference isochron, while the 10 Ma reference isochron is also drawn in as a guide to the two outliers.*

DISCUSSION

Primary Ore Samples

Snelling[31] has already highlighted a telling omission by Hills and Richards.[32] Having included all the Pb isotopic ratios they had obtained on their five uraninite samples, they tabulated also the derived 'ages', except for those obtainable from ^{208}Pb (see Table 6 again). Since their data table lists the necessary ingredients for ^{208}Pb 'age' calculations — the %Th, ^{208}Pb proportion, and $^{208}Pb/^{207}Pb$ and $^{208}Pb/^{204}Pb$ ratios — their omission of the ^{208}Pb 'ages' is both conspicuous and significant. These Th-derived 'dates' should normally be regarded as the most reliable, since Th is less mobile in geochemical environments and therefore open system

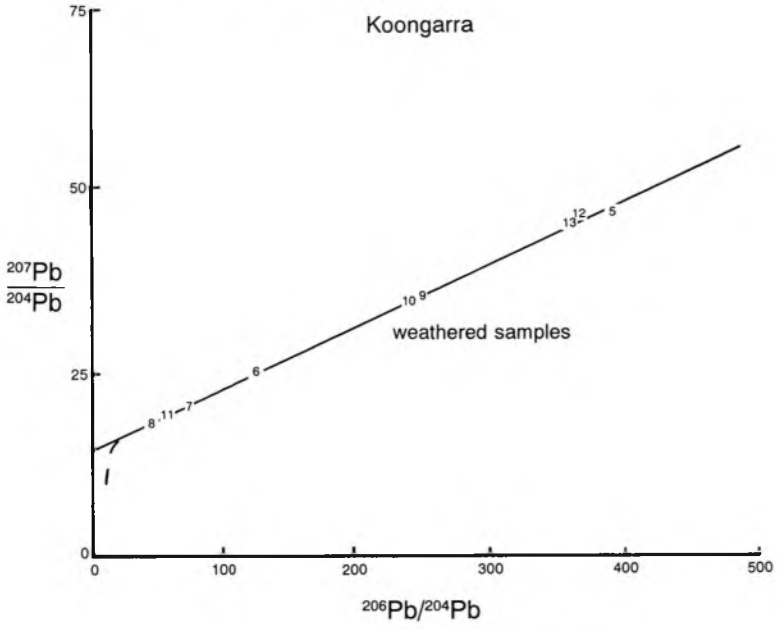

Figure 25. *A conventional $^{207}Pb/^{204}Pb$ vs $^{206}Pb/^{204}Pb$ isochron diagram showing all the weathered whole-rock samples plotting as a linear array which gives an apparent isochron 'age' of 1270 ±50 Ma. (This diagram is an expansion of the lower left hand corner of Figure 23.)*

behaviour is less likely than for U.

The ^{204}Pb content of the uraninite is regarded as 'common' or original Pb since it is not derived from any parent element via radioactive decay. Because this so-called 'common' Pb is also believed to carry a significant quantity of the ^{206}Pb, ^{207}Pb and ^{208}Pb isotopes, a 'common' Pb correction has to be applied to the raw data before calculation of the U-Th-Pb 'ages'. This, of course, is an admission that not all the quantities of these Pb isotopes are derived by radioactive decay, some being with the U and Th 'in the beginning'. The standard used to correct the data in Table 6 was the Mt Isa Pb standard with an isotopic composition:–

1.44% ^{204}Pb	23.20% ^{206}Pb
22.48% ^{207}Pb	52.88% ^{208}Pb

It should be noted in passing also that the choice of this standard is based on one of several **theories** of element nucleogenesis and Pb isotopic evolution,[33,34] making the whole 'age' calculation procedure rather subjective, based on further assumptions.

When this 'common' Pb correction is applied to the data in Table 6,[35] most of the ^{208}Pb has resulted from 'common' Pb contamination. In fact, in samples J804/1, J804/b and J807 all the ^{208}Pb is due to contamination and none to ^{232}Th decay, thus resulting in ^{208}Pb 'ages' of 0 Ma (within the experimental/analytical errors) for these samples. The remaining two samples yield ^{208}Pb 'ages'[36] of 275 Ma (J801) and 61 Ma (J809), both considerably less than all other Pb 'ages'. Since they are as valid as any of the other resultant 'ages' calculated, these $^{232}Th/^{208}Pb$ 'ages' should have been at least reported (one suspects they were left out of the tabulated results because of the uncomfortable implications). After all, the $^{232}Th/^{208}Pb$ 'age' of 0 Ma is the only Pb isotopic 'date' from that study supported directly by a majority of samples (three out of the five), and Th-derived 'dates' should be reliable as the ^{232}Th decay chain is a standard isotopic 'clock', but a 0 Ma 'age' makes little more sense than their 870 Ma 'age' from the U-Pb data. In any case, Hills and Richards' 'age' of 1700–1800 Ma for the first generation of U mineralisation at Koongarra neither fits the geological criteria for an expected 1550–1600 Ma 'age', nor does their 870 Ma 'date' correlate with any geological event capable of remobilising U and Pb to produce the presumed second generation of U mineralisation.

Using the procedure of Ludwig,[37] standard $^{207}Pb/^{206}Pb$ diagrams were prepared for the uraninite, galena and whole-rock data sets, and combinations thereof, to check the regression statistics and possible derived 'isochrons' using the standard York[38] method. In each case the mean square of weighted deviates (MSWD), which tests the 'goodness of fit' of data to a line, is large to extremely large, which reflects in the derived isochron 'ages' of 841 ±140 Ma (uraninites), 1008 ±420 Ma (galenas), 668 ±330 Ma (whole-rocks), 818 ±150 Ma (uraninites plus galenas) and 863 ±130 Ma (all three data

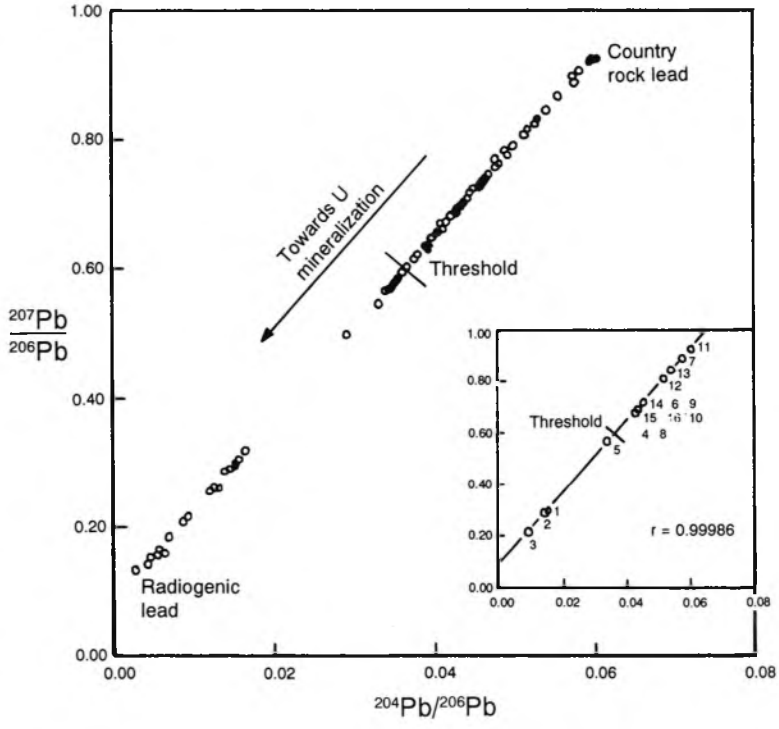

Figure 26. *Plot of $^{207}Pb/^{206}Pb$ vs $^{206}Pb/^{204}Pb$ for all 113 soil samples from the Koongarra area analysed by Dickson* et al., *indicating the high correlation of r = 0.99986 between the two variables with a fitted regression line yielding an apparent isochron 'age' of 1445 ±20 Ma. The insert shows the distribution of samples about a threshold dividing radiogenic Pb and country rock Pb along this proposed mixing line.*

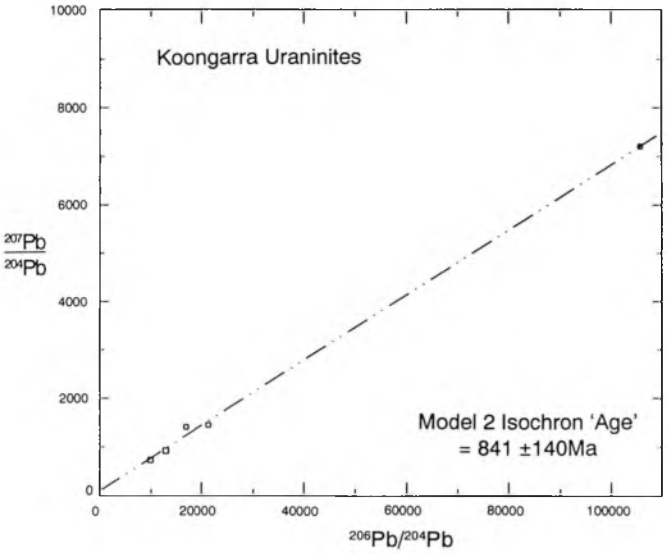

Figure 27. *A conventional $^{207}Pb/^{204}Pb$ vs $^{206}Pb/^{204}Pb$ diagram with all Koongarra uraninites plotted on it using Ludwig's ISOPLOT program and defining an apparent isochron with a model 2 'age' of 841 ±140 Ma.*

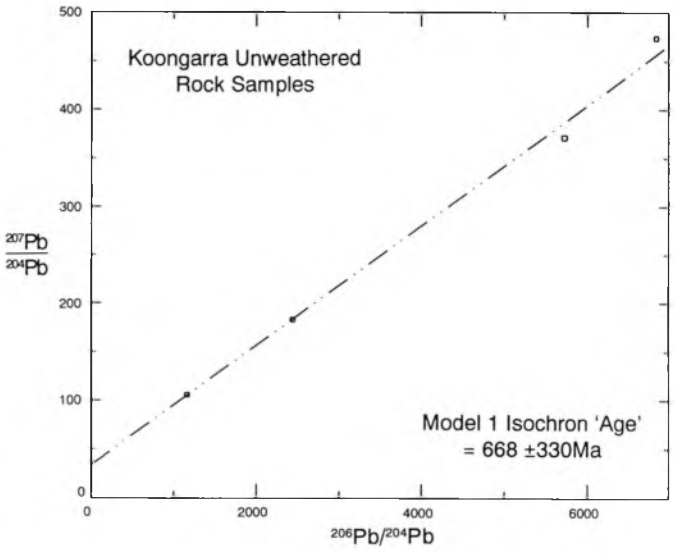

Figure 29. *A conventional $^{207}Pb/^{204}Pb$ vs $^{206}Pb/^{204}Pb$ diagram with all the unweathered whole-rock samples from Koongarra plotted on it using Ludwig's ISOPLOT program and defining an apparent isochron with a model 1 'age' of 668 ±330 Ma.*

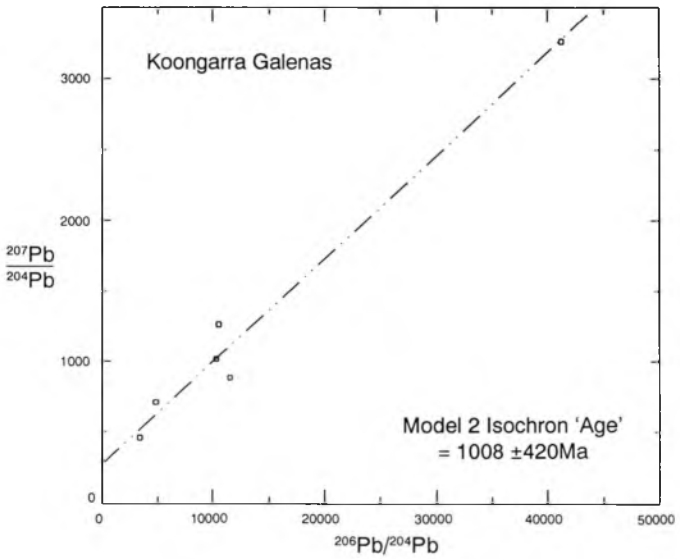

Figure 28. *A conventional $^{207}Pb/^{204}Pb$ vs $^{206}Pb/^{204}Pb$ diagram with all Koongarra galenas plotted on it using Ludwig's ISOPLOT program and defining an apparent isochron with a model 2 'age' of 1008 ±420 Ma.*

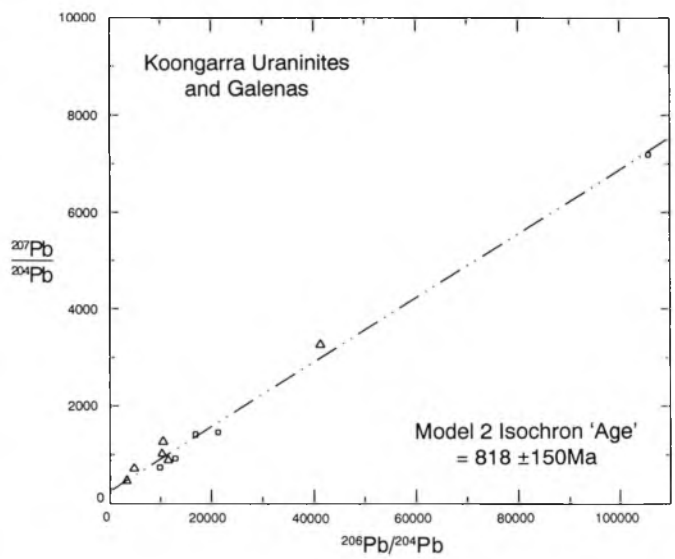

Figure 30. *A conventional $^{207}Pb/^{204}Pb$ vs $^{206}Pb/^{204}Pb$ diagram with both the Koongarra uraninites and galenas plotted on it using Ludwig's ISOPLOT program and defining an apparent isochron with a model 2 'age' of 818 ±150 Ma.*

sets combined), all 'ages' being within the 95% confidence limits (see Figures 27–31). It is perhaps fortuitously significant that the combination of all three data sets yields an isochron 'age' of 863 ±130 Ma, almost identical to Hills and Richards' near-concordant 'age' of 862 Ma, although this was using a line-fitting routine of Ludwig[39] that assigns equal weights and zero error-correlations to each data point to avoid the mistake of weighting the points according to analytical errors when it is clear that some other cause of scatter is involved, which is clearly the case here. The normal York[40] algorithm assumes that the only cause for scatter from a straight line are the assigned errors, and for the combined data set here the amount of scatter calculated thereby yields an astronomical MSWD of 669000 and a bad line of fit that yields an isochron 'age' of 1632 ±410 Ma (see Figure 32). This 'result' may make more geological sense, but the regression statistics are such that derivation of any 'age' information from these data is totally unjustified, even though it can be rightfully argued that these samples form a cogenetic set (they are all samples of U ore or its components from the

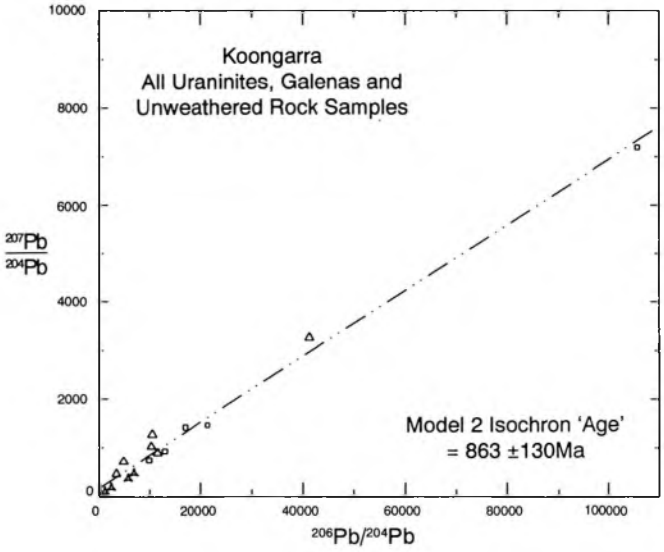

Figure 31. *A conventional $^{207}Pb/^{204}Pb$ vs $^{206}Pb/^{204}Pb$ diagram with all Koongarra uraninites, galenas and unweathered whole-rock samples plotted on it using Ludwig's ISOPLOT program and defining an apparent isochron with a model 2 'age' of 863 ±130 Ma.*

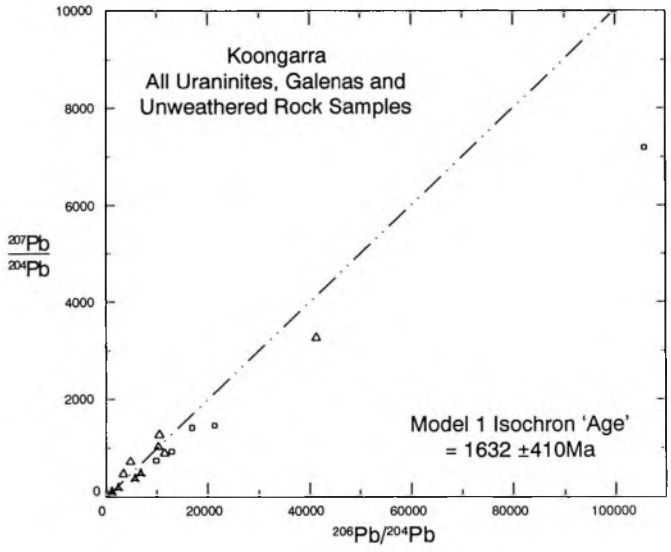

Figure 32. *A conventional $^{207}Pb/^{204}Pb$ vs $^{206}Pb/^{204}Pb$ diagram with all Koongarra uraninites, galenas and unweathered whole-rock samples plotted on it using Ludwig's ISOPLOT program and defining an apparent isochron with a model 1 'age' of 1632 ± 410 Ma but an enormous scatter.*

same primary ore zone at Koongarra).

It is not uncommon to find that 'ages' derived from standard $^{207}Pb/^{206}Pb$ plots are erroneous, even though the data fit well-defined linear arrays ('isochrons'). Ludwig *et al.*[41] found that this was due to migration of both Pb and radioactive daughters of ^{238}U yielding a $^{207}Pb/^{206}Pb$ 'isochron' giving *'superficially attractive results which would nonetheless be seriously misleading'* because the derived 'age' (in their example) was more than six times higher than the U-Pb isochron 'age'. Similarly, Cunningham *et al.*[42] obtained $^{207}Pb/^{206}Pb$ isochron 'ages' up to 50 times higher than those derived from 'more reliable' U-Pb isochrons for whole-rock U ore samples, even though *'the apparent slight degree of scatter is almost entirely a misleading artifact'*. Likewise, at Jabiluka, an almost identical style of uranium deposit in the identical geological setting only about 60 km due north of Koongarra, Gulson and Mizon[43] had considerable difficulty obtaining Pb-Pb and U-Pb isochron 'ages' for the U mineralisation due to ^{238}U daughter leakage and diffusion out of the U minerals and ore into the surrounding host rocks and constituent minerals, that therefore had gained excess radium (Ra) and ^{206}Pb. Ironically, at Koongarra the U-Pb isochron using Ludwig[44] on Hills and Richards' uraninite data yields an 'age' of 857 ±149 Ma (with an MSWD of 13400, tolerably large compared to that obtained with the Pb-Pb isochron) (see Figure 33), almost identical to the 'fortuitous' Pb-Pb isochron 'age' obtained using Ludwig's modified algorithm on the combined three data sets (863 ±130 Ma), as well as Hills and Richards' single near-concordant 862 Ma 'age'.

As has already been described, Snelling and Dickson[45] have demonstrated that there is significant uranium/daughter disequilibrium in the primary ore and surrounding host rocks at Koongarra due to the redistribution of both U and its Ra decay product, just as Gulson and Mizon found at Jabiluka. That Ra mobility at depth in the primary ore zone is currently more significant than U migration has been confirmed by Dickson and Snelling,[46] which of course results ultimately in the redistribution of ^{206}Pb, the end-member of the whole ^{238}U decay chain. Dickson *et al.*[47] have demonstrated that Ra is

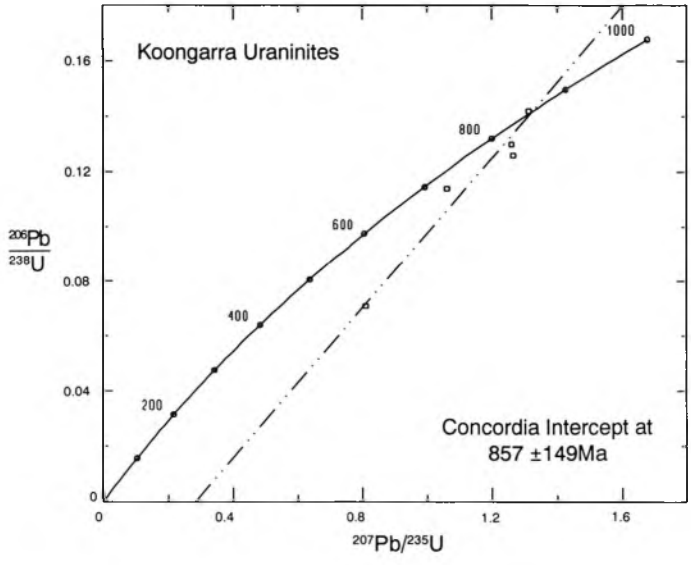

Figure 33. *A conventional $^{206}Pb/^{238}U$ vs $^{207}Pb/^{235}U$ concordia diagram with all the Koongarra uraninites plotted on it using Ludwig's ISOPLOT program and defining an apparent isochron that intersects concordia at 857 ±149 Ma.*

transported through the unweathered rocks in this area in the ground waters, while Davy *et al.*[48] have determined the emanation rate of radon (Rn) gas from the Koongarra No. 1 orebody, an ever present hazard in uranium ore mining operations. The Rn gas is known to migrate along fractures and rise through the ground over considerable distances to form a halo in the air above, while Rn is also transported in ground waters. Thus it is to be expected that the pattern of oxidation of uraninites and dispersion of U should reflect the present-day circulation of ground waters[49] and that present-day ground waters should be carrying U and He.[50,51] Such groundwater dispersion of U and mobility of Ra has, of course, resulted in U and Pb dispersion into the surrounding soils,[52] where the Pb isotopic signature of the U ore is clearly evident.[53,54]

These observations alone demonstrate the open system behaviour of the U-Th-Pb system that renders meaningless any 'age' information derived. However, both Hills[55] and Snelling[56] have recognised that U and Pb also have migrated several times and on a considerable scale in the primary ore zone, with the latest redistribution having produced supergene uraninites, often with colloform banding, found as fracture and cavity infillings (see Figure 16 again), and between quartz and gangue grain boundaries. The unit cell dimensions of these uraninites, plus this textural evidence, supports the conclusion that these uraninites have precipitated after dissolution of earlier formed uraninite and transportation in low-temperature ground waters. With such wholesale repeated migrations of U also, all attempts at 'dating' must be rendered useless, especially when whole-rock samples, in which different generations of uraninites are lumped together, are used. Indeed, it must surely be virtually impossible to be certain of the precise status and history of any particular piece of uraninite selected for 'dating'. Even though every conceivable precaution is taken when selecting grains for 'dating', how can we be sure that the U and Pb isotopes and isotopic ratios measured represent the 'original', unaffected by the gross element movements for which there is such abundant evidence? The uraninite grains or ore samples 'dated' always contain radiogenic Pb both within crystal lattices of minerals, and as microscopic inclusions or grains and veins of galena, but how can we be sure all the Pb was generated by radioactive decay from U *in situ*? In any case, the uraninite grains and veins do not have uniform compositions — either between or within grains — so that 'dating' of sub-sections of any grain or vein would be expected to yield widely divergent U-Pb and Pb-Pb ratios and therefore 'ages' even within that single grain or vein. Thus it is logical to conclude, as others have already,[57-59] that U-Th-Pb ratios may have little to do with the 'ages' of many minerals, rocks and ores.

Weathered Rocks and Soils

In contrast to the poor-fitting linear arrays produced from the Pb-Pb data of minerals and whole-rocks from the primary ore zone, that all appear to give an apparent (false) isochron 'age' grouped around 857–863 Ma, both Carr and Dean[60] and Dickson *et al.*[61] found that weathered schist whole-rock and soil samples produced good fitting linear arrays that would normally represent 'isochrons' that yield 'ages' of 1270 Ma and 1445 Ma respectively (see Figures 25 and 26 again). The weathered whole-rock samples all of course come from Koongarra itself, and consist of secondary ore samples from the weathered schist zone, plus weathered schist samples that contain U dispersed down-slope by ground waters moving through the weathered rock. Because these whole-rock samples come from a volume of rock through which U is known to be migrating, leading to redistribution not only of U but of its decay products, it is therefore very surprising to find that these whole-rock samples define a good enough linear array to yield an 'isochron'. Even the observed scatter calculated using Ludwig[62] is much less than that associated with fitting an 'isochron' to the ^{207}Pb-^{206}Pb data from the primary ore zone samples, which is again surprising given U migration in the weathered zone, the data from which one would expect to show considerable scatter and thus no 'age' consensus. Furthermore, it is baffling as to why the 'isochron'-derived 'age' (1270 Ma) of the weathered secondary ore zone should be so much 'older' than the 'isochron'-derived 'age' (857–863 Ma) of the primary ore, which of course is ultimately the source through weathering and groundwater transport of the U, decay products and the stable Pb isotopes that are in the secondary and dispersed ore. Perhaps the only explanation is that the 'isochron' represents the mixing of radiogenic Pb from the mineralisation with the 'common' or background Pb in the surrounding schists, which are even in a relative sense older than the U mineralisation.

The idea of such an 'isochron' being a mixing line was suggested by Dickson *et al.*[63] They were, however, dealing with the Pb isotopic data obtained from soil samples collected from depths of only about 30–40 cm, the majority of which represented sandy soils consisting of detritus eroded from the Kombolgie sandstone. For this mixing explanation to be feasible there should be some other evidence of mobilisation of Pb in the area. Dickson *et al.* found that not only were there high $^{206}Pb/^{204}Pb$ ratios in three of their soil samples from the near-surface (0–1 m) zone south of the No. 1 orebody in the hydrogeochemical halo, but there was a lack of any other U-series daughter products in the same samples. This near-surface zone is inundated for approximately six months of the year as a result of the high monsoonal rainfall in this tropical area. Towards the end of the ensuing six-month dry season the water table has been known to drop in some cases more than ten metres from its wet season 'high'. This means that the top of the weathered schist zone is regularly fluctuating between wet and dry conditions, so that any trace elements such as Pb leached from the weathered ore and transported by ground water in the weathered schist zone would also be dispersed vertically up into the thin surficial sand cover on top of the weathered schist — the sandy soils that were sampled by Dickson *et al.*[64,65] Snelling[66] found that

Pb was a significant pathfinder element for uranium ore in the Koongarra environment, anomalous Pb being present in the surficial sand cover above the zone of weathered primary ore, and that there was even hydrodynamic dispersal of Pb at a depth of 0.5–1.5 m. Dickson *et al.*[67] found a similarity between the isotopic ratios for Pb extracted from their soil samples by either a mild HCl-hydroxylamine (pH 1) or a strong 7*M* HCl-7*M* HNO_3 leach, which indicates that Pb is loosely attached to sand grain surfaces in the samples rather than tightly bound in silicate or resistate mineral lattices. This in turn suggests Pb is adsorbed from ground waters, meaning that radiogenic Pb is being added to the 'common' or background Pb in the sand by both vertical and lateral groundwater dispersion.

However, not all of Dickson *et al.*'s soil samples came from the area immediate to the Koongarra orebodies, nor were they all samples of Kombolgie sandstone detritus. That this mixing line explanation for the apparent 'isochron' is clearly demonstrated for these samples from the immediate Koongarra area is not in question, although it is somewhat surprising that these soil samples should give an apparent isochron 'age' (1445 Ma) somewhat older than that obtained from the weathered schist samples beneath (1270 Ma). Indeed, the 'common' or background Pb in the respective samples should reflect an 'older' apparent age in the schists compared to the sandstone, due to their relative ages based on the geological relationship between them. (Remember, the schists are supposed to be the product of regional metamorphism at 1800–1870 Ma, while the Kombolgie sandstone is regarded as having been deposited around 1600–1680 Ma.) However, the apparent ages are the other way around, the sandy soils from the Kombolgie sandstone detritus yielding an 'older' apparent age (1445 Ma) compared to that yielded by the weathered schists (1270 Ma). Perhaps this difference is a reflection of the extent of mixing in each type of sample at their respective levels in the weathering profile. Nevertheless, what is astounding is that Dickson *et al.*[68] found that even though several of their soil samples consisted of weathered schist or basement granite (containing accessory zircon) up to 17 km from the known U mineralisation, they still plotted on the same apparent 'isochron'. Indeed, the 'fit' is comparatively good (see Figure 34), as indicated by the MSWD of only 964 using Ludwig,[69] yet much of this observed scatter can be attributed to two samples out of the 113, one of which was subsequently found to be probably contaminated by cuttings from an adjacent drill hole.[70] If that sample is removed from the regression analysis the MSWD drops to 505, indicating that almost half of the observed scatter is due to that one data point alone. If the data point that is the next worst for fitting to the apparent 'isochron' is removed, then the MSWD drops by a further 315 to a mere 190. Yet in both cases the apparent 'isochron' or 'mixing line' still has lying on or close to it the samples from up to 17 km away from the known U mineralisation **and** the samples that are not Kombolgie sandstone detritus. The final 'isochron' fitted to the remaining 111 samples still yields an 'age' of 1420 ±18 Ma (see Figure 34 again).

While Carr and Dean's nine weathered schist whole-rock samples are not strictly cogenetic with Dickson *et al.*'s 113 soil samples, the two sample sets are obviously related because the source of the radiogenic Pb in the majority of the soil samples from the immediate Koongarra area is the same as that in the weathered schists. Not surprisingly, when the regression analysis was performed on Carr and Dean's nine weathered schist whole-rock samples using Ludwig,[71] the MSWD for the observed scatter was 24100, indicating a

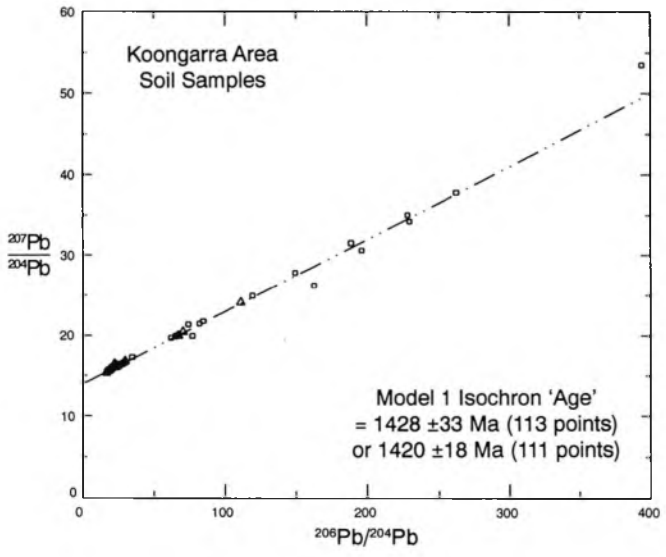

Figure 34. *A conventional $^{207}Pb/^{204}Pb$ vs $^{206}Pb/^{204}Pb$ diagram with all Koongarra area soil samples plotted on it using Ludwig's ISOPLOT program and defining an apparent isochron with a model 1 'age' of 1428 ±33 Ma for all 113 samples and 1420 ±18 Ma for 111 samples (2 outliers removed).*

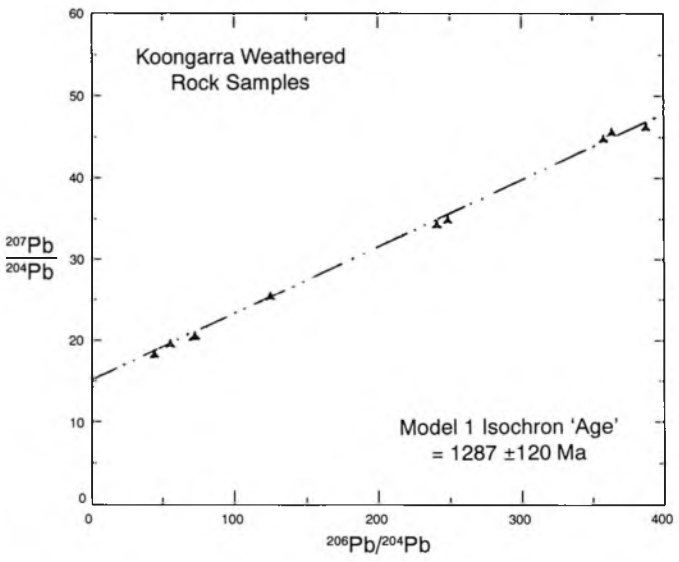

Figure 35. *A conventional $^{207}Pb/^{204}Pb$ vs $^{206}Pb/^{204}Pb$ diagram with the weathered whole-rock samples from Koongarra plotted on it using Ludwig's ISOPLOT program and defining an apparent isochron with a model 1 'age' of 1287 ±120 Ma.*

poor fit to an 'isochron' which yielded an 'age' of 1287 ±120 Ma (see Figure 35). Yet when these nine samples were added to the 113 soil samples the MSWD dropped substantially to 1210, and not surprisingly the fitted 'isochron' yielded an 'age' of 1346 ±27 Ma, an 'isochron age' intermediate between those of the two data sets being combined (see Figure 36). However, when the two soil samples responsible for the majority of the scatter in that data set were removed the MSWD dropped to 430 and yielded an 'isochron age' of 1336 ±17 Ma (see Figure 36 again).

General Comments

As with all the other apparent isochron 'ages', these results from the weathered rocks and soils have no apparent geological meaning, because there is no geological event to which these 'ages' might correlate. Indeed, even in the evolutionary time-frame the weathering of the Koongarra U mineralisation is extremely recent, and in any case, these 'ages' derived from Pb-Pb 'isochrons' from the weathered rock and soil samples are much 'older' than the supposedly more reliable U-Pb 'isochron age' of the Koongarra primary ore. But since that latter result has no apparent geological meaning, because it also cannot be correlated with any known geological event, nothing then is certain at all from any of these U-Th-Pb isotopic studies of the Koongarra ores, rocks and surrounding soils. Indeed, it is just as certain that the primary ore is 0 Ma, based on three $^{232}Th/^{208}Pb$ single sample ages, as is the claim that one near-concordant result means that there was formation of Pb-free uraninite at 870 Ma. After all, this postulated formation of Pb-free uraninite is supposed to have occurred in an environment where there

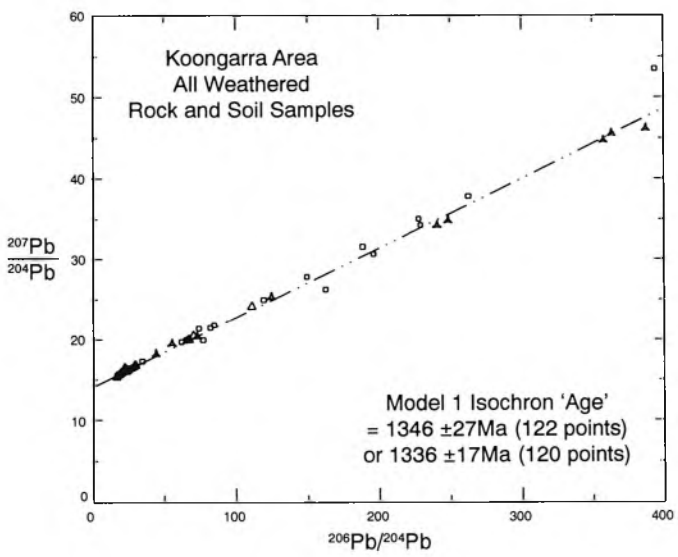

Figure 36. *A conventional $^{207}Pb/^{204}Pb$ vs $^{206}Pb/^{204}Pb$ diagram with all Koongarra area weathered whole-rock and soil samples plotted on it using Ludwig's ISOPLOT program and defining an apparent isochron with a model 1 'age' of 1346 ± 27 Ma for all 122 samples and 1336 ± 17 Ma for 120 samples (2 outliers removed).*

was Pb left over from an earlier 1700–1800 Ma original U mineralisation for which we no longer have any evidence, textural or otherwise, apart from a rather tenuous interpretation of Pb isotopic evidence that has otherwise shown itself to be devoid of any capability of providing any 'age' information.

All these results raise serious fundamental questions about the claimed validity of the U-Th-Pb 'dating' method. It may seem reasonable to regard an apparent 'isochron' as a 'mixing line' within the restricted area close to the known source of radiogenic Pb, which can be shown by independent evidence to be migrating into rocks and soils that contain 'common' or background Pb in the immediate environs. However, it strains all credulity to suggest that a false 'isochron' through a data set derived from samples representing a variety of rock types, of significantly different evolutionary 'ages', over an area of up to 17 km lateral extent from the known radiogenic Pb source, can still represent mixing! One can only conclude that all assumptions used to derive the estimates of 'common' or background Pb, including models for the supposed evolution of the stable Pb isotopes through earth history, from their presumed commencement on the protoearth with its claimed original Pb isotope content some 4.6 billion or so years ago, cannot be valid. Equally, we cannot be sure what the U-Th-Pb system's isotopic ratios really mean, because the basic assumptions that are foundational to the interpretation of these isotopic ratios are fatally flawed. Not only has open system behaviour of these isotopes been demonstrated as the norm, but even where there is an apparent 'isochron' with an excellent 'goodness of fit' the derived 'age' is invariably geologically meaningless.

Thus creationists need not be hindered in building their Creation-Flood young-earth model for the geological record by the many claims in the open geological literature that U-Th-Pb radiometric 'dating' has 'proved' the presumed great antiquity of the earth, and the strata and fossils of the so-called geological column. Accordingly, all the apparent isochron and other 'ages' that have been referred to here have been quoted as millions of years (Ma) purely in order to reveal the shortcomings of the U-Th-Pb 'dating' method. Indeed, even the use of conventional geological era terms such as 'Archaean' and 'Lower Proterozoic' has been for convenient reference to the rock units under discussion, there being no absolute 'age' significance attached to these terms here — only a relative position within the overall rock record. There is clearly a real sequence of rock units that comprise the total geological record, from the so-called Archaean to the Recent, the formation of which needs to be understood and coherently modelled within the biblical framework of a recent Creation and global Flood. Much progress towards this goal has been, and is being, made within the relatively small creationist geological community. Thus the mounting evidence that the claimed 'absolute dating' methods, such as U-Th-Pb radiometrics, are unreliable at best, and in reality produce many results that are impressive but geologically meaningless, can only assist in this quest.

CONCLUSIONS

The concerns raised by Zheng[72] regarding U-Pb isochrons are warranted. At Koongarra a $^{207}Pb/^{206}Pb$ 'isochron' produced from 11 hand-picked uraninite and galena grains, plus four whole-rock samples, yields an 'age' of 863 Ma, the same as a near-concordant 'age' of 862 Ma from one of the uraninite grains. Nine weathered whole-rock samples yield an 'isochron age' of 1270 Ma, while 113 soil samples produce an excellent 'isochron' with an 'age' of 1445 Ma. All of these 'ages' are geologically meaningless. While the apparent isochron produced by the soil samples may be identified as a mixing line, produced by the mixing of radiogenic Pb with 'common' or background Pb in the surrounding rocks and soils, even this explanation strains credulity because the samples come from up to 17 km away from known U mineralisation, and a few of the soil samples represent different rock types. Not only then has open system behaviour of these isotopes been demonstrated, as confirmed by the independent evidence of ore textures, mineral chemistry, supergene alteration, uranium/daughter disequilibrium, and groundwater and soil geochemistry, but apparent 'isochrons' and their derived 'ages' are invariably geologically meaningless. Thus none of the assumptions used to interpret the U-Th-Pb isotopic system to yield 'ages' can be valid. If these assumptions were valid, then the $^{232}Th/^{208}Pb$ 'age' of 0 Ma for three of the five uraninite samples should be taken seriously. Creationists should therefore not be intimidated by claims that U-Th-Pb radiometric 'dating' has 'proved' the presumed great antiquity of the earth, and the strata and fossils of the so-called geological column.

REFERENCES

1. Zheng, Y.-F., 1989. Influences of the nature of the initial Rb-Sr system on isochron validity. **Chemical Geology, 80**:1–16 (p. 14).
2. Needham, R. S. and Stuart-Smith, P. G., 1980. Geology of the Alligator Rivers Uranium Field. *In*: **Uranium in the Pine Creek Geosyncline**, J. Ferguson and A. B. Goleby (eds), International Atomic Energy Agency, Vienna, pp. 233–257.
3. Needham, R. S., 1984. Alligator River, Northern Territory — 1:250,000 Geological Series. **Bureau of Mineral Resources, Geology and Geophysics Australia**, Explanatory Notes, SD 53-1.
4. Needham, R. S., 1988. Geology of the Alligator Rivers Uranium Field, Northern Territory. **Bureau of Mineral Resources, Geology and Geophysics Australia, Bulletin 224**, Canberra, Australia.
5. Snelling, A. A., 1990. Koongarra uranium deposits. *In*: **Geology of the Mineral Deposits of Australia and Papua New Guinea**, F. E. Hughes (ed.), The Australasian Institute of Mining and Metallurgy, Melbourne, Australia, pp. 807–812.
6. Johnston, J. D., 1984. **Structural Evolution of the Pine Creek Inlier and Mineralisation Therein, Northern Territory, Australia**, Ph.D. thesis (unpublished), Monash University, Melbourne, Australia.
7. Snelling, A. A., 1980. Uraninite and its alteration products, Koongarra uranium deposit. *In*: **Uranium in the Pine Creek Geosyncline**, J. Ferguson and A. B., Goleby (eds), International Atomic Energy Agency, Vienna, pp. 487–498.
8. Page, R. W., Compston, W. and Needham, R. S., 1980. Geochronology and evolution of the Late-Archaean basement and Proterozoic rocks in the Alligator Rivers Uranium Field, Northern Territory, Australia. *In*: **Uranium in the Pine Creek Geosyncline**, J. Ferguson and A. B. Goleby (eds), International Atomic Energy Agency, Vienna, pp. 39–68.
9. Maas, R., 1987. **The Application of Sm-Nd and Rb-Sr Isotope Systematics to Ore Deposits**, Ph.D. thesis (unpublished), The Australian National University, Canberra, Australia.
10. Maas, R., 1989. Nd-Sr isotope constraints on the age and origin of unconformity-type uranium deposits in the Alligator Rivers Uranium Field, Northern Territory, Australia. **Economic Geology, 84**:64–90.
11. Airey, P. L., Golian, C. and Lever, D. A., 1986. An approach to the mathematical modelling of the uranium series redistribution within ore bodies. **Topical Report AAEC/C49**, Australian Atomic Energy Commission, Sydney.
12. Hills, J. H., 1973. **Lead Isotopes and the Regional Geochemistry of North Australian Uranium Deposits**, Ph.D. thesis (unpublished), Macquarie University, Sydney, Australia.
13. Snelling, A. A., 1980. **A Geochemical Study of the Koongarra Uranium Deposit, Northern Territory, Australia,** Ph.D. thesis (unpublished), The University of Sydney, Sydney, Australia.
14. Snelling, Ref. 13.
15. Snelling, Ref. 7.
16. Snelling, A. A. and Dickson, B. L., 1979. Uranium/daughter equilibrium in the Koongarra uranium deposit, Australia. **Mineralium Deposita, 14**:109–118.
17. Dickson, B. L. and Snelling, A. A., 1980. Movements of uranium and daughter isotopes in the Koongarra uranium deposit. *In*: **Uranium in the Pine Creek Geosyncline**, J. Ferguson and A. B. Goleby (eds), International Atomic Energy Agency, Vienna, pp. 499–507.
18. Giblin, A. M. and Snelling, A.A., 1983. Application of hydrogeochemistry to uranium exploration in the Pine Creek Geosyncline, Northern Territory, Australia. **Journal of Geochemical Exploration, 19**:33–55.
19. Gole, M. J., Butt, C. R. M. and Snelling, A. A., 1986. A groundwater helium survey of the Koongarra uranium deposits, Pine Creek Geosyncline, Northern Territory. **Uranium, 2**:343–360.
20. Snelling, A. A., 1984. A soil geochemistry orientation survey for uranium at Koongarra, Northern Territory. **Journal of Geochemical Exploration, 22**:83–99.
21. Dickson, B. L., Gulson, B. L. and Snelling, A. A., 1985. Evaluation of lead isotopic methods for uranium exploration, Koongarra area, Northern Territory, Australia. **Journal of Geochemical Exploration, 24**:81–102.
22. Dickson, B. L., Gulson, B. L. and Snelling, A. A., 1987. Further assessment of stable lead isotope measurements for uranium exploration, Pine Creek Geosyncline, Northern Territory, Australia. **Journal of Geochemical Exploration, 27**:63–75.
23. Hills, J. H. and Richards, J. R., 1972. The age of uranium mineralization in Northern Australia. **Search, 3**:382–385.
24. Hills, J. H. and Richards, J. R., 1976 Pitchblende and galena ages in the Alligator Rivers Region, Northern Territory, Australia. **Mineralium Deposita, 11**:133–154.
25. Hills and Richards, Ref. 24.
26. Carr, G. R. and Dean, J. A., 1986. **Report to AAEC on a Pb Isotopic Study of Samples from Jabiluka and Koongarra**, Unpublished Report, Commonwealth Scientific and Industrial Research Organisation, Division of Mineral Physics and Mineralogy, Sydney.
27. Carr and Dean, Ref. 26.
28. Dickson *et al.*, Ref. 21.
29. Dickson *et al.*, Ref. 22.
30. Dickson *et al.*, Ref. 22.
31. Snelling, A. A., 1981. The age of Australian uranium: a case study of the Koongarra uranium deposit. **Ex Nihilo, 4**:44–57.
32. Hills and Richards, Ref. 24.
33. Faure, G., 1986. The isotope geology of lead. *In*: **Principles of Isotope Geology**, 2nd edition, John Wiley and Sons, New York, Chapter 19, pp. 309–340.
34. Dalrymple, G. B., 1991. Isotopes of lead: the hourglass of the solar system. *In*: **The Age of the Earth**, Stanford University Press, Stanford, California, Chapter 7, pp. 305–356.
35. Stieff, L. R., Stern, T. W., Oshiro, S. and Senftle, F. E., 1959. **Tables for the Calculation of Lead Isotope Ages**, US Geological Survey, Professional Paper 334A.
36. Stieff *et al.*, Ref. 35.
37. Ludwig, K. R., 1993. **ISOPLOT: A Plotting and Regression Program**

for Radiogenic-Isotope Data, Version 2.60, United States Geological Survey, Open-File Report 91-445, Denver, Colorado.
38. York, D., 1969. Least-squares fitting of a straight line with correlated errors. **Earth and Planetary Science Letters, 5**:320–324.
39. Ludwig, Ref. 37.
40. York, Ref. 38.
41. Ludwig, K. R., Nash, J. T. and Naeser, C. W., 1981. U-Pb isotope systematics and age of uranium mineralisation, Midnite Mine, Washington. **Economic Geology, 76**:89–110.
42. Cunningham, C. G., Ludwig, K. R., Naeser, C. W., Weiland, E. K., Mehnert, H. H., Steven, T. A. and Rasmussen, J. D., 1982. Geochronology of hydrothermal uranium deposits and associated igneous rocks in the eastern source area of the Mount Belknap Volcanics, Marysvale, Utah. **Economic Geology, 77**:453–463.
43. Gulson, B. L. and Mizon, K. J., 1980. Lead isotope studies at Jabiluka. *In*: **Uranium in the Pine Creek Geosyncline**, J. Ferguson and A. B. Goleby (eds), International Atomic Energy Agency, Vienna, pp. 439–455.
44. Ludwig, Ref. 37.
45. Snelling and Dickson, Ref. 16.
46. Dickson and Snelling, Ref. 17.
47. Dickson, B. L., Giblin, A. M. and Snelling, A. A., 1987. The source of radium in anomalous accumulations near sandstone escarpments, Australia. **Applied Geochemistry, 2**:385–398.
48. Davy, D. R., Dudaitis, A. and O'Brien, B. G., 1978. Radon survey at the Koongarra uranium deposit, Northern Territory. Topical Report AAEC/E459, Australian Atomic Energy Commission, Sydney. *In*: **Koongarra Project: Draft Environmental Impact Statement**, Noranda Australia Limited, Melbourne, Appendix 2.
49. Snelling, Ref. 7.
50. Giblin and Snelling, Ref. 18.
51. Gole *et al.*, Ref. 19.
52. Snelling, Ref. 20.
53. Dickson *et al.*, Ref. 21.
54. Dickson *et al.*, Ref. 22.
55. Hills, Ref. 12.
56. Snelling, Ref. 13.
57. Gentry, R. V., Christie, W. H., Smith, D. H., Emery, J. F., Reynolds, S. A., Walker, R., Cristy, S. S. and Gentry, P. A., 1976. Radiohalos in coalified wood: new evidence relating to the time of uranium introduction and coalification. **Science, 194**:315–318.
58. Kazmann, R. G., 1978. It's about time: 4.5 billion years. **Geotimes, 23**(9):18–20.
59. Kazmann, R. G., 1979. Time: in full measure. **Eos, 60**(2):19–22.
60. Carr and Dean, Ref. 26.
61. Dickson *et al.*, Ref. 22.
62. Ludwig, Ref. 37.
63. Dickson *et al.*, Ref. 22.
64. Dickson *et al.*, Ref. 21.
65. Dickson *et al.*, Ref. 22.
66. Snelling, Ref. 20.
67. Dickson *et al.*, Ref. 21.
68. Dickson *et al.*, Ref. 22.
69. Ludwig, Ref. 37.
70. Dickson *et al.*, Ref. 21.
71. Ludwig, Ref. 37.
72. Zheng, Ref. 1.

Dr Andrew Snelling is a geologist with a B.Sc. (Hons) from The University of New South Wales and a Ph.D. from The University of Sydney. He has worked in the mining industry and is still a consultant geologist in the field and in research projects, but now also works full-time with the Creation Science Foundation where he contributes to **Creation Ex Nihilo** magazine and edits the **Creation Ex Nihilo Technical Journal**. He resides in Brisbane, Australia.